nature communications

Article

https://doi.org/10.1038/s41467-024-54620-4

A vaccine platform targeting lung-resident memory CD4$^+$ T-cells provides protection against heterosubtypic influenza infections in mice and ferrets

Received: 7 February 2024

Accepted: 18 November 2024

Published online: 29 November 2024

Check for updates

Kwang Hyun Ko[1,2], Hyun Shik Bae[1], Jeong Woo Park[2,3], Jin-Sun Lee[2,3], Somin Park[3], Jun Heo[4], Hyunsoo Park[4], Jaeseok Choi[5], Eunseo Bae[5], Woonsung Na[5], Seong-Hyun Park[6], Baik-Lin Seong[7], Seung Hyun Han[2,3], Dong-Ho Kim[1,8] ✉ & Seung Bin Cha[1,8] ✉

Lung tissue-resident memory T (T_{RM}) cells induced by influenza vaccination are crucial for heterosubtypic immunity upon re-exposure to the influenza virus, enabling rapid and robust responses upon reactivation. To enhance the efficacy of influenza vaccines, we induce the generation of lung T_{RM} cells following intranasal vaccination with a commercial influenza vaccine adjuvanted with NexaVant (NVT), a TLR3 agonist-based adjuvant. We demonstrate that intranasal immunization with the NVT-adjuvanted vaccine provides improved protection against influenza virus infections by inducing the generation of CD4$^+$ T_{RM} cells in the lungs in a type I interferon-dependent manner. These pulmonary CD4$^+$ T_{RM} cells provide potent mucosal immunity and cross-protection against heterosubtypic infections in both mouse and ferret models. This vaccine platform has the potential to significantly improve conventional intramuscular influenza vaccines by providing broader protection.

Seasonal influenza, an acute respiratory illness that is highly contagious, still poses a considerable global threat[1]. Vaccination is considered one of the most cost-efficient and effective strategies for preventing influenza illness[2,3]. To date, most influenza vaccines are designed to control influenza viruses by producing neutralizing antibodies specific for hemagglutinin (HA) and neuraminidase (NA)[3]. However, these surface proteins are highly variable due to antigenic drift and shift, and antibody-based immunity has limitations in preventing infection caused by variants or pandemic viruses that are not antigenically matched[3,4]. Thus, current influenza vaccines, which mainly provide strain-specific immunity, have significant limitations in protection against novel strains resulting from the constant evolution of influenza viruses[5,6]. Therefore, the development of a novel vaccine capable of providing long-lasting protection with broad coverage in the respiratory tract is needed.

[1]R&D Center, NA Vaccine Institute, Seoul 05854, Republic of Korea. [2]Interdisciplinary Program in Genetic Engineering, College of Natural Sciences, Seoul National University, Seoul 08826, Republic of Korea. [3]Department of Oral Microbiology and Immunology, and Dental Research Institute, School of Dentistry, Seoul National University, Seoul 08826, Republic of Korea. [4]Vaccine R&D Team, Central Institute, Il-Yang Pharmaceutical, Yongin 17096, Republic of Korea. [5]College of Veterinary Medicine, Chonnam National University, Gwangju 61186, Republic of Korea. [6]Graduate Program in Biomaterials Science and Engineering, College of Life Science and Biotechnology, Yonsei University, Seoul 08826, Republic of Korea. [7]Department of Microbiology and Immunology, Yonsei University College of Medicine, Seodaemun-gu, Seoul 08826, Republic of Korea. [8]These authors contributed equally: Dong-Ho Kim, Seung Bin Cha. ✉e-mail: dhk@navaccine.org; sbcha@navaccine.org

One strategy for vaccine development against infectious diseases is to mimic natural infection[7]. Recently, this approach was applied to design a vaccine for coronavirus disease 2019 (COVID-19), a respiratory infectious disease whose emergence led to a worldwide pandemic. Compared to traditional parenteral vaccines, intranasal administration of the COVID-19 vaccine has shown improved protective efficacy against not only vaccine strains but also variant strains[8]. In this way, if local immunity is induced by targeting the natural route of infection, various types of immune sentinels, such as mucosal immunity and resident memory T (T_{RM}) cells, can be recruited at the site of infection[9]. In particular, recent researches on the generation of pulmonary T_{RM} cells and their contribution to the control of respiratory pathogens, which has received much public attention due to the COVID-19 pandemic, have recently been intensively reviewed[9–12].

Lung T_{RM} cells provide remarkable protection against infection with influenza virus, especially heterosubtypic strains that escape from preexisting neutralizing antibodies[12,13]. Thus, developing vaccines that induce pulmonary T_{RM} cells to target influenza would be a good approach for long-term prevention of various influenza virus infections[12]. To date, the development of targeting T_{RM} cells in the lung has mostly been studied in individuals who were naturally infected and subsequently recovered[14–16] or in parabiosis models[17–19]. In addition, most studies on vaccines targeting the respiratory tract are conducted using viral vectors or live-attenuated viruses[20–24]. In particular, despite recent clinical studies in which viral vectors were used as vaccines for targeting the respiratory tract, which failed to induce sufficient mucosal immunity[25], research on vaccines utilizing a subunit vaccine platform involving the use of adjuvants remains limited. Furthermore, most studies on lung T_{RM} cells involve $CD8^+$ T_{RM} cells generated from model antigens or specifically known CD8 epitopes in mice[21,26,27]. Although MHC-II is highly expressed on the surface of lung epithelial cells[28], which is a favorable niche for $CD4^+$ T-cell responses and excessive induction of $CD8^+$ T_{RM} cells might cause immunopathology[29–31], research on the formation and role of $CD4^+$ T_{RM} cells in the respiratory tract is still lacking.

NexaVant (NVT) is a TLR3 agonist recently developed by our research team[32,33]. It is a substance that overcomes several drawbacks of existing poly(I:C) and its derivatives, such as heterogeneity and problems in quantitation, qualification, stability and safety. When administered in vivo, NVT induces an innate immune response by producing type I interferon (IFN) and activating dendritic cells (DCs) and can be used as an adjuvant for vaccines. In this study, we hypothesized that NVT could be used as a vaccine platform by mimicking a viral infection and inducing immune responses in the respiratory tract when it is codelivered to the lungs with an antigen.

To test this hypothesis, we evaluated the profile of the immune responses generated when NVT was simply mixed with a commercially available influenza vaccine and subsequently delivered to the lungs, the target organ of influenza. When the vaccine was delivered to the lung, a humoral response similar to that of the vaccine administered intramuscularly occurred but also additional mucosal immunity and cell-mediated immune responses were induced; these responses were not induced by the intramuscularly injected vaccine. Furthermore, it was confirmed that $CD4^+$ T_{RM} cells in the lung contribute to protection against influenza viruses of other subtypes. In particular, among the induced $CD4^+$ T_{RM} population, the presence or absence of specific cross-reactivity to the nucleoprotein (NP) included in the vaccine was essential for cross-protection. The formation of a lung $CD4^+$ T_{RM} population by the vaccine was dependent on the type I IFN induced by the NVT in the vaccine, and it was confirmed that at least during booster vaccination, codelivery of antigen and adjuvant to the lungs is essential for T_{RM} cell formation. Finally, we verified this principle of cross-protection in ferrets, a model animal for influenza. The results reveal the role of this vaccine platform in the cross-protective mechanism of influenza through the formation of lung $CD4^+$ T_{RM} cells.

Results

Intranasal vaccination with NVT-adjuvanted quadrivalent influenza vaccine (QIV) provides superior protection against homologous virus challenge

First, we investigated whether adding NVT to the influenza vaccine or delivering the vaccine to the lungs via the intranasal route could improve the efficacy of the conventional injectable influenza vaccine. BALB/c mice were immunized intramuscularly (*i.m.*) with QIV or intranasally (*i.n.*) with QIV or NVT-adjuvanted QIV (QIV + NVT) twice at two-week intervals, and immune response analysis and challenge were performed two weeks after the last immunization (Fig. 1a). Intramuscular injection of QIV induced serum antibody responses as expected, while intranasal administration of QIV elicited minimal antibody responses (Fig. 1b, c). Intranasal administration of QIV + NVT induced QIV-specific total IgG and IgG1 antibody responses at levels higher than those elicited by intramuscular injection of QIV. The addition of NVT to the vaccine effectively promoted QIV-specific IgG2a production compared to that of the vaccine alone (Fig. 1b). Furthermore, intranasal administration of QIV + NVT-induced QIV-specific IgA in nasal washes and bronchoalveolar lavage fluid (BALF), which was not induced by intramuscular injection of QIV (Fig. 1c).

Next, lung and spleen cells from the vaccinated mice were stimulated with QIV, after which Th1 (IFN-γ^+CD4^+ T-cells), Th2 (IL-4^+CD4^+ T-cells), Th17 (IL-$17A^+CD4^+$ T-cells) and cytotoxic T lymphocyte (CTL, IFN-γ^+CD8^+ T-cells) responses were analyzed using flow cytometry. Intranasal administration of QIV was not sufficient to induce T-cell responses in either the lung or spleen, whereas intramuscular injection of QIV induced some T-cell responses in the spleen (Fig. 1d). We found that intranasal immunization with QIV + NVT elicited robust Th1 responses in both the lung and spleen (Fig. 1d) but did not induce Th2, Th17, or CTL responses (Supplementary Fig. 1). This finding suggested that the addition of NVT to influenza vaccines contributes to influenza-specific Th1 responses, as evidenced by IgG isotype switching. In fact, NVT strongly promoted DC activation and the migration of innate immune cells in draining lymph nodes (Supplementary Fig. 2), and it is likely that this activation of the innate immune system contributed to the T-cell response.

To evaluate the efficacy of the vaccine against homosubtypic viral challenge, vaccinated mice were infected *i.n.* with 100 or 5000 lethal dose $(LD)_{50}$ of the H1N1 influenza virus. When challenged with 100 LD_{50} of H1N1 virus, mice injected *i.m.* with QIV exhibited initial weight loss but recovered and survived, whereas all mice administered QIV *i.n.* died. Meanwhile, mice injected *i.m.* with QIV had a survival rate as low as 20% when challenged with 5000 LD_{50} of the virus. Mice vaccinated with *i.n.* QIV + NVT were protected against H1N1 virus challenge without significant weight change (Fig. 1e, f). Taken together, these findings suggest that the use of NVT as an adjuvant is essential for improving the efficacy of influenza vaccines, and intranasal administration of NVT-adjuvanted vaccines provides superior protective immunity by promoting both mucosal IgA and $CD4^+$ T-cell responses. Since intranasal administration of antigen alone did not induce an immune response, this vaccine group was excluded from further experiments.

Intranasal immunization with the NVT-adjuvanted H3N2 vaccine provides cross-protection against H1N1 virus challenge

Immune mediators such as mucosal IgA and $CD4^+$ T-cells have been reported to induce cross-protection[34]. Therefore, we explored whether lung delivery of an NVT-adjuvanted vaccine via the intranasal route could contribute to protection against heterosubtypic virus challenge. To test this hypothesis, BALB/c mice were immunized *i.m.* with H3N2

https://doi.org/10.1038/s41467-024-54620-4

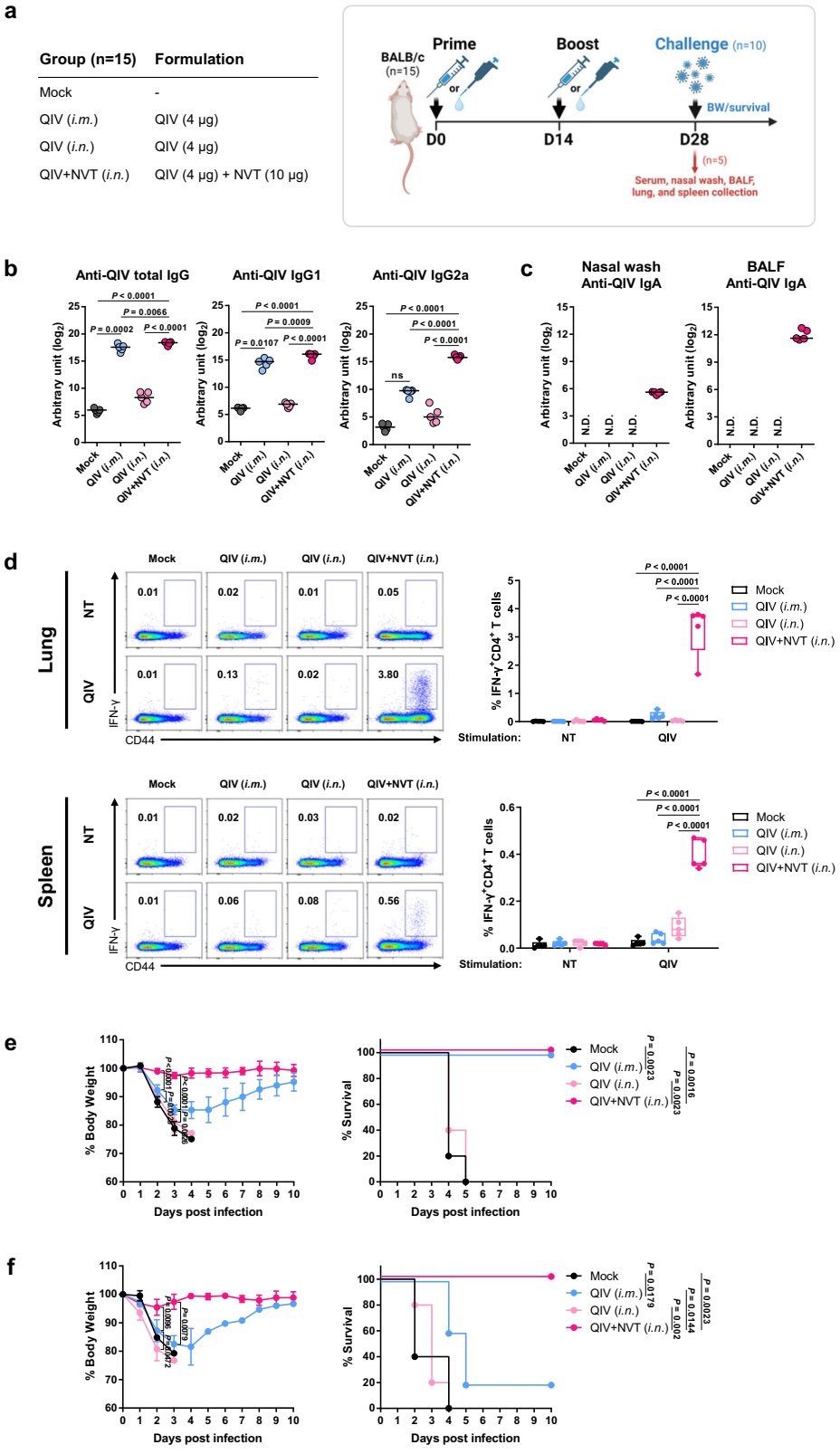

or *i.n.* with NVT-adjuvanted H3N2 (H3N2 + NVT) twice at two-week intervals. Two weeks after the last immunization, the hemagglutination inhibition (HAI) antibody and T-cell response were examined (Fig. 2a). We found that both vaccine groups produced serum HAI antibodies against the vaccine strain H3N2 but not against the heterosubtypic H1N1 strain. The intranasal administration of H3N2 + NVT also induced the production of HAI antibodies against H3N2 but not H1N1 in nasal washes or BALF, indicating that the vaccine could induce only strain-specific neutralizing antibodies (Fig. 2b). Regarding cellular immunity, intranasal immunization with H3N2 + NVT elicited a $CD4^+$ T-cell response to H1N1 as well as H3N2 in both the lung and spleen, whereas intramuscular injection of H3N2 did not induce $CD4^+$ T-cell responses (Fig. 2c). To further determine whether cross-reactive T-cells could contribute to protection against heterosubtypic influenza

Fig. 1 | Intranasal administration of QIV in combination with NVT provides superior protection against homologous influenza virus challenge. **a** Experimental design. BALB/c mice (n = 15 per group) were immunized *i.m.* with QIV or *i.n.* with QIV or QIV + NVT twice at two-week intervals. Two weeks after the last immunization, immune response analysis (n = 5 per group) (**b**–**d**) and H1N1 virus (A/Korea/2785/2009) challenge (n = 10 per group) (**e**, **f**) were performed. Schematic image was created in BioRender. Han, S. (2024) BioRender.com/d59a368. **b**, **c** (**b**) QIV-specific total IgG, IgG1, and IgG2a in the serum and (**c**) QIV-specific IgA in the nasal wash and BALF were assessed via ELISA. The data are expressed as dot plots, with horizontal lines representing the medians. **d** After stimulating lung and spleen cells with QIV, the IFN-γ$^+$CD4$^+$ T-cell response was determined by flow cytometry. Box and whisker plots show the median (center), 25th and 75th percentiles (box), and lowest and highest values (whiskers). **e**, **f** The vaccinated mice were infected *i.n.* with (**e**) 100 LD_{50} (n = 5 per group) or (**f**) 5000 LD_{50} (n = 5 per group) of H1N1 virus, and body weight and survival were monitored daily. Weight-loss data are shown as mean value ± standard deviation (SD). Survival data are represented as Kaplan–Meier survival curves, and the significant differences in survival rates were calculated by the log-rank test. **b**-**f** Statistical analyses were performed using one-way ANOVA with Tukey's multiple comparisons test or two-sided Mann–Whitney U test. This study was performed independently at least three times, and one representative set is shown. BW body weight; N.D. not detected; ns, not significant; NT non-treated. Source data are provided as a Source Data file.

virus in the absence of neutralizing antibodies, vaccinated mice were infected with a lethal dose (4 LD_{50}) of H1N1 virus. Mice injected *i.m.* with H3N2 did not survive. In contrast, mice administered H3N2 + NVT via the intranasal route experienced weight loss but fully recovered and survived (Fig. 2d). To confirm viral load reduction and histopathological recovery in the lungs, lung viral loads were measured at 3 and 6 days post infection (dpi), and lung histopathology was analyzed at 6 dpi. Mice administered H3N2 + NVT intranasally showed a dramatic reduction in lung viral load over time compared to intramuscularly injected mice, which displayed no decrease in lung viral titers (Fig. 2e). Furthermore, severe lung damage was observed in the *i.m.* injected and mock groups, whereas mild inflammatory changes were observed in the mice immunized *i.n.* with H3N2 + NVT (Fig. 2f and Supplementary Fig. 3). Finally, to avoid concerns that protection may be primarily driven by innate cells due to the two doses of vaccine and the short period of 2 weeks after vaccination, we administered the vaccine at 4-week intervals, as is common in humans, and performed immune response analysis and challenge 4 weeks after the last vaccination. As a result, we found that both the 2-week and 4-week interval vaccination schedules induced comparable levels of protective immunity (Supplementary Fig. 4). Overall, intranasal immunization with H3N2 + NVT confers broad protection through the induction of cross-reactive memory CD4$^+$ T-cells.

Memory CD4$^+$ T-cells contribute to protection against heterosubtypic influenza virus infection

To assess whether vaccine-induced CD4$^+$ T-cells directly contribute to heterosubtypic protection, mice administered H3N2 + NVT *i.n.* were treated with the monoclonal antibody GK1.5 (anti-CD4) three times before viral challenge to remove CD4$^+$ T-cells (Fig. 3a). At the time of challenge, the number of CD4$^+$ T-cells in both the lung and spleen was specifically decreased (Fig. 3b). Nasal wash IgA antibodies produced after vaccination were maintained even when CD4$^+$ T-cells were depleted (Fig. 3c). Moreover, vaccine-induced HAI antibodies were not disrupted by CD4$^+$ T-cell depletion (Fig. 3d). Finally, the cross-protection obtained by intranasal immunization with H3N2 + NVT was abolished when CD4$^+$ T-cells were depleted (Fig. 3e). Therefore, memory CD4$^+$ T-cells, not antigen-specific mucosal IgA antibodies, elicited by intranasal vaccination with H3N2 + NVT play a crucial role in heterosubtypic immunity and protection.

Lung CD4$^+$ T_{RM} cells play a critical role in heterosubtypic protection

Through previous studies, we confirmed that the CD4$^+$ T-cell response is essential for cross-protection. However, mRNA vaccines, which were first used for COVID-19 prevention, are administered *i.m.*; the vaccine administration route effectively induces cellular immune responses, including CD4$^+$ T-cell responses[35]. Nevertheless, mRNA vaccines also show limited effectiveness against COVID-19 variants[36]; moreover, due to this obstacle, booster shots or bivalent vaccines have been developed and used. In light of this, we hypothesized that the CD4$^+$ T-cell response induced by the vaccine would also differ depending on the route of vaccine administration, and we conducted the following experiment to verify this hypothesis. Considering that intramuscular injection of the NVT-adjuvanted vaccine induces CD4$^+$ T-cell responses in the spleen[32], BALB/c mice were immunized *i.m.* with H3N2 or H3N2 + NVT, or *i.n.* with H3N2 + NVT twice at two-week intervals (Fig. 4a). Two weeks after the last vaccination, intramuscular injection of H3N2 did not induce CD4$^+$ T-cell responses in either the lung or spleen, whereas intranasal administration of H3N2 + NVT induced CD4$^+$ T-cell responses to H1N1 and H3N2 in both the lung and spleen (Fig. 4b). Intramuscular injection of H3N2 + NVT induced CD4$^+$ T-cell responses in the spleen to a comparable extent as intranasal administration of H3N2 + NVT but lower CD4$^+$ T-cell responses in the lung (Fig. 4b). In the absence of neutralizing antibodies against H1N1 (Fig. 4c), infection with a lethal dose of H1N1 virus demonstrated that splenic CD4$^+$ T-cell responses were not sufficient for cross-protection and that pulmonary CD4$^+$ T-cell responses were essential for heterosubtypic protection (Fig. 4d). Given that lung CD4$^+$ T_{RM} cells are key to protection against multiple variants[37], we further analyzed the subsets of T-cells in the lung using flow cytometry. The abundance of CD4$^+$ T_{RM} cells (CD4$^+$CD44$^+$CD62L$^-$CD69$^+$) was significantly increased in the lungs of mice administered H3N2 + NVT via the intranasal route. Most of the lung CD4$^+$ T_{RM} population derived in this study consisted of CD103$^-$ cells. (Fig. 4e). Even though a slight lung CD4$^+$ T-cell response was observed in the group administered H3N2 + NVT *i.m.*, the group did not exhibit the induction of lung CD4$^+$ T_{RM} cells. Meanwhile, lung CD8$^+$ T_{RM} cells (CD8$^+$CD44$^+$CD62L$^-$CD69$^+$) were not observed. We also found that the lung CD4$^+$ T_{RM} population was maintained at 20 months after vaccination and contributed to cross-protection (Supplementary Fig. 5). Taken together, these findings suggest that the NVT-adjuvanted intranasal influenza vaccine offers long-term and broad protection against respiratory infection by various influenza virus strains through the induction of a lung CD4$^+$ T-cell response.

Type I IFN signaling is essential for the induction of protective immunity by the NVT-adjuvanted intranasal influenza vaccine

When double-stranded RNA (dsRNA), such as NVT, acts on corresponding RNA sensors in the host, it first induces the production of type I IFN. Because NVT effectively promotes IFN-β production[32], we investigated whether the protective immunity induced by the NVT-adjuvanted vaccine depends on type I IFN signaling. To explore this hypothesis, we considered the fact that IFNAR1$^{-/-}$ mice are known to be highly susceptible to various strains of influenza virus[38]. Thus, wild-type (WT) or IFNAR1$^{-/-}$ (KO) mice were immunized *i.n.* with H3N2 + NVT, and KO mice were immunized *i.m.* with H1N1 to demonstrate that IFNAR1-deficient mice can also be protected from infection if they have vaccine strain-specific antibodies (Fig. 5a). In addition, the KO mock group was used to confirm the similarity between the KO and WT groups during influenza virus infection (Fig. 5a). We found that even in KO mice, intramuscular vaccination with H1N1 induced sufficient serum HAI antibodies to protect against influenza (Fig. 5b). However, in the intranasal immunization of H3N2 + NVT, the HAI titer of serum and nasal wash was significantly decreased in KO mice compared to that in WT mice (Fig. 5b, c). Moreover, in KO mice, lung CD4$^+$ T_{RM} cells

https://doi.org/10.1038/s41467-024-54620-4

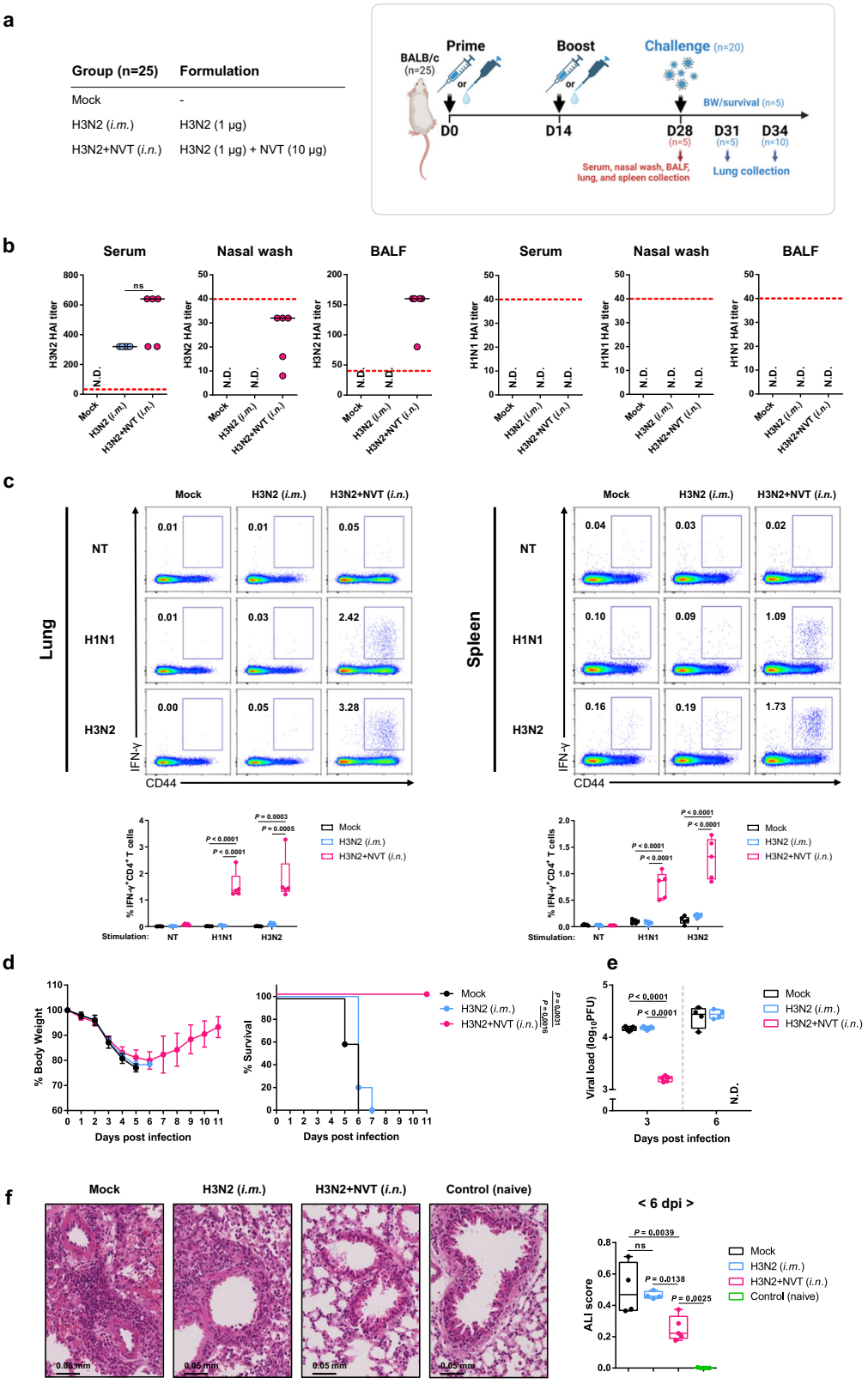

were not generated, and lung memory CD4$^+$ T-cell responses to H1N1 and H3N2 were not induced (Fig. 5d, e). Finally, KO mice immunized *i.m.* with H1N1 and WT mice immunized *i.n.* with H3N2 + NVT survived challenge with a lethal dose of H1N1 virus, whereas KO mice immunized with H3N2 + NVT did not. Therefore, type I IFN signaling is critical for the cross-protective effects of the NVT-adjuvanted intranasal influenza vaccine.

The NVT-induced CCL2, CCL5, and CXCR3/ligand axis contributes to lung CD4$^+$ T_{RM} cell formation, but direct codelivery of antigens is essential

Lung T_{RM} cells develop as effector memory T-cells migrate to the respiratory tract and differentiate functionally and phenotypically in an optimal cytokine milieu[9]. Given that lung T_{RM} development is impaired in mice lacking type I IFN signaling (Fig. 5d), we sought to

Fig. 2 | Intranasal immunization with NVT-adjuvanted H3N2 confers cross-protection against lethal heterosubtypic influenza virus challenge. **a** Experimental design. BALB/c mice (n = 25 per group) were immunized *i.m.* with H3N2 or *i.n.* with H3N2 + NVT twice at two-week intervals. Two weeks after the last immunization, immune response analysis (n = 5 per group) (**b**, **c**) and H1N1 virus (A/Korea/2785/2009) challenge (n = 20 per group) (**d**–**f**) were performed. Schematic image was created in BioRender. Han, S. (2024) BioRender.com/b04n737. **b** HAI antibody titers against H3N2 or H1N1 in serum, nasal wash, and BALF were measured via HAI assay. An HAI antibody titer of 1:40 (red dotted line) was considered protective against influenza infection. The data are expressed as dot plots, with horizontal lines representing the medians. **c** After stimulating lung and spleen cells with H1N1 or H3N2, the IFN-γ^+CD4$^+$ T-cell response was determined by flow cytometry. **d**–**f** The vaccinated mice were infected *i.n.* with 4 LD_{50} of H1N1 virus. **d** Body weight and survival (n = 5 per group) were monitored daily. Weight-loss data are shown as mean value ± SD. Survival data are represented as Kaplan–Meier survival curves, and the significant differences in survival rates were calculated by the log-rank test. **e** On days 3 and 6 after the challenge, lung viral loads were assessed using a plaque assay (n = 5 per group). **f** On day 6 after the challenge, lung tissues from mice (n = 5 per group) were collected, and histological sections of vaccinated and control (naïve) mice were stained with hematoxylin and eosin. Acute lung injury (ALI) scores of sectioned lungs. A score of zero indicates healthy lungs, whereas a score of one signifies severe acute lung injury. **c**, **e**, **f** Box and whisker plots show the median (center), 25th and 75th percentiles (box), and lowest and highest values (whiskers). **b**–**f** Statistical analyses were performed using one-way ANOVA with Tukey's multiple comparisons test or two-sided Mann–Whitney U test. This study was performed independently at least three times, and one representative set is shown. BW body weight, N.D. not detected, ns not significant, NT non-treated. Source data are provided as a Source Data file.

determine which chemokines and cytokines are influenced by type I IFN signaling. To explore this, WT and IFNAR1$^{-/-}$ mice were immunized *i.n.* with H3N2 + NVT, after which the levels of chemokines and cytokines in lung homogenates and serum were measured using a cytokine array kit, and the results were confirmed by ELISA. The results showed that CCL2, CCL5, CXCL9, and CXCL10 levels were significantly reduced in IFNAR1$^{-/-}$ mice (Fig. 6a, b). We also found that these chemokines are induced by NVT rather than by the antigen (Fig. 6c). These chemokines are all known to be related to T-cell migration[39–41]. Previous reports have shown that the chemokines CXCL9 and CXCL10 can be applied as a strategy for pulling circulating effector T-cells to local sites for T_{RM} development[42]. We next investigated whether memory CD4$^+$ T-cells primed systemically by an *i.m.* administered vaccine could be trafficked to the lungs by NVT. To better induce a systemic T-cell response, NVT was also included in the intramuscular administration group. Compared to that in the group that did not receive NVT, the lung CD4$^+$ T_{RM} population tended to increase slightly. However, the formation of lung CD4$^+$ T_{RM} cells was lower than in the intranasal H3N2 + NVT group (Fig. 6d), and cross-protection was not observed (Fig. 6e). We subsequently conducted the following experiment to determine the requirements for inducing CD4$^+$ T_{RM} cells via our vaccine. It is known that local cognate antigens are essential for CD8$^+$ T_{RM} formation[9]. To confirm whether antigen recognition is essential for CD4$^+$ T_{RM} cells to be induced by the vaccine or whether both antigen and inflammatory signals elicited by NVT are required, we examined how CD4$^+$ T_{RM} cells are formed in response to various prime/boost regimens. As a result, CD4$^+$ T_{RM} cells were formed only when the antigen and NVT were codelivered in the booster shot, regardless of the type of vaccine administered during the priming vaccination (Fig. 6f). These findings indicate that pulmonary CD4$^+$ T_{RM} cells can develop after one booster shot in people who have previously been vaccinated by intramuscular injection.

The influenza NP is a major source of CD4 epitopes for cross-protective immunity conferred by the NVT-adjuvanted intranasal influenza vaccine

The majority of the currently used influenza vaccines are split-virus or subunit vaccines, and they contain both HA and NP[43]. In particular, the HA stem and NP are highly conserved viral proteins targeted for cross-protective T-cell immunity against different viral subtypes[44,45]. The vaccine antigens used in this study were drug substances obtained from a commercially available inactivated split influenza vaccine, so they contained both HA and NP (Supplementary Fig. 6). To determine which components of the NVT-adjuvanted influenza vaccine contribute to broad protection, BALB/c mice were immunized *i.n.* with NVT-adjuvanted recombinant H3N2 HA (H3N2 rHA), recombinant H3N2 NP (H3N2 rNP), or H3N2 from the split influenza vaccine (Fig. 7a). We found that none of the components of the H3N2 vaccine were associated with antibody-mediated neutralization of the H1N1 virus (Fig. 7b, c). Moreover, regardless of the components of the vaccine, CD4$^+$ T_{RM} formation in the lungs was similar in all groups (Fig. 7d). Regarding the T-cell response, intranasal immunization with H3N2 rNP, but not H3N2 rHA, induced lung CD4$^+$ T-cell responses against H1N1, although these responses were lower than those observed following vaccination with the whole H3N2 protein (Fig. 7e). In addition, the HA protein induced a CD4$^+$ T-cell response in the group vaccinated with the same subtype but did not induce cross-reactivity in the other subtypes. (Fig. 7e). To further explore whether cross-reactive CD4$^+$ T-cells induced by H3N2 rNP provide heterosubtypic protection, vaccinated mice were challenged with a lethal dose of H1N1 virus. Mice given H3N2 rHA did not survive H1N1 infection, whereas mice vaccinated with H3N2 NP survived (Fig. 7f). Therefore, for cross-protection, not only must CD4$^+$ T_{RM} cells be formed, but the resulting CD4$^+$ T_{RM} cells must be specific for the target antigen. In this vaccine, the CD4$^+$ T-cell epitopes that induce cross-reactivity between heterosubtypic strains were confirmed to be present in the NP.

NVT-adjuvanted intranasal vaccines provide broad protection in a variety of cases

Previously, we described the principle of cross-protection induced by this vaccine platform between only subtypes H1N1 and H3N2 of influenza virus. Therefore, we wondered whether this principle could apply to other subtypes and confirmed this through the following experiment. In the case of influenza B viruses, not only do the vaccines not produce cross-protective antibodies between the two lineages (BV and BY) but they also do not induce cross-protective antibodies against influenza type A, so they are also used separately as drug substances in commercial QIV. First, we investigated whether the NVT-adjuvanted influenza vaccine could contribute to cross-protection within type B or between type A and type B influenza viruses. To explore this possibility, mice were immunized *i.m.* with BV or BY, or *i.n.* with BY + NVT and infected with a lethal dose of BV virus. The results showed that mice administered BY + NVT via the intranasal route survived the BV challenge, exhibiting superior protection compared to mice given BV via the intramuscular route (Fig. 8a). As in the case of H1N1 and H3N2, a cross-reaction between BV and BY was also observed in the T-cell response analysis (Supplementary Fig. 7a). Meanwhile, mice immunized *i.n.* with BY + NVT did not survive the lethal dose of H1N1 virus challenge (Supplementary Fig. 7b). Although lung CD4$^+$ T_{RM} cells were formed in the group vaccinated *i.n.* with BV + NVT, they did not cross-react with H1N1; thus, cross-protection failed (Supplementary Fig. 7b, c). To further examine whether the NVT-adjuvanted influenza vaccine provides protection against viruses of other origins, mice were immunized with human H3N2 + NVT and challenged with canine H3N2 virus. As a result, mice vaccinated *i.n.* with H3N2 + NVT initially lost weight but recovered, and all the mice that survived while vaccinated *i.m.* with H3N2 showed a low survival rate, as expected (Fig. 8b).

In 2009, influenza H1N1 pdm09, originating in pigs, emerged as the first pandemic of the 21st century, and it incapacitated the efficacy of influenza vaccines used at the time[46]. We hypothesized that we

https://doi.org/10.1038/s41467-024-54620-4

a

Group (n=8)	Formulation
Mock	-
H3N2 (*i.m.*)	H3N2 (1 μg)
H3N2+NVT (*i.n.*) + isotype	H3N2 (1 μg) + NVT (10 μg)
H3N2+NVT (*i.n.*) + αCD4	H3N2 (1 μg) + NVT (10 μg)

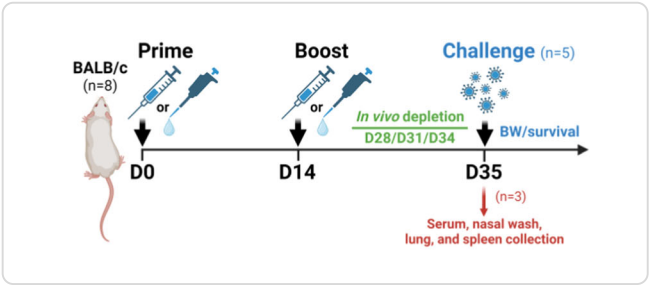

b

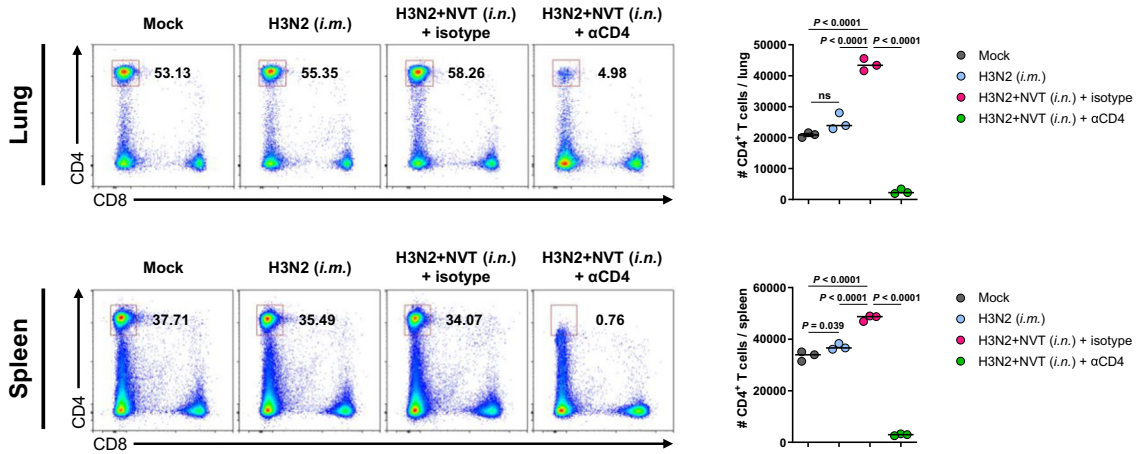

c

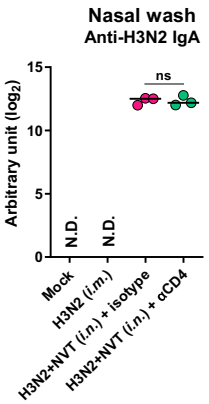

d

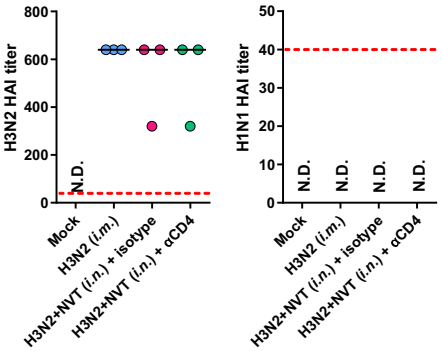

e

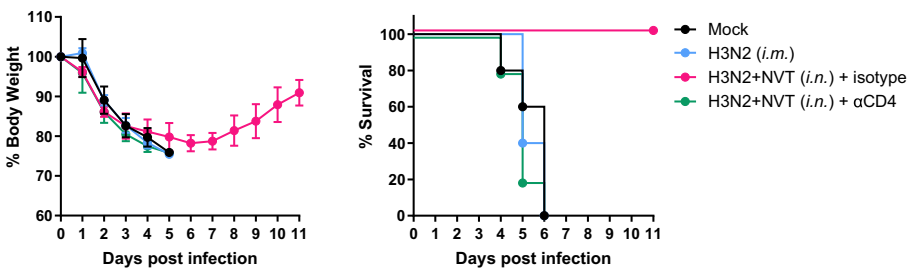

would have been able to protect against H1N1 pdm09 if we had access to appropriate vaccines at that time, and we conducted subsequent experiments to verify this hypothesis. However, since a vaccine containing the non-H1N1 pdm09 strain is not currently available, the currently used QIV was administered as a vaccine and animals were challenged with the non-pdm09 strain PR8 (A/Puerto Rico/8/1934 H1N1). We found that all the mice administered QIV *i.m.* died as previously described[46], whereas the mice administered QIV + NVT *i.n.* survived challenge infection (Fig. 8c).

Influenza not only causes pandemics such as pdm09 but also has severe mutations due to antigenic drift[2]. Therefore, current influenza vaccines are produced using different strains selected through predictions each year and administered yearly[2]. For this reason, the effectiveness of these vaccines also varies depending on the mismatch

Fig. 3 | CD4⁺ T-cell responses play a critical role in protection against heterosubtypic virus infection. a Experimental design. BALB/c mice were immunized *i.m.* with H3N2 (n = 8) or *i.n.* with H3N2 + NVT (n = 16) twice at two-week intervals. Two weeks after the last immunization, H3N2 + NVT-administered mice were treated with an isotype control (n = 8) or a GK1.5 (anti-CD4) monoclonal antibody (n = 8) three times for one week. Then, immune response analysis (n = 3 per group) (**b**–**d**) and H1N1 virus (A/Korea/2785/2009) challenge (n = 5 per group) (**e**) were performed. Schematic image was created in BioRender. Han, S. (2024) BioRender.com/t11y924. **b** Depletion of CD4⁺ T-cells in the lung and spleen was confirmed using flow cytometry. **c** H3N2-specific IgA in nasal washes was assessed via ELISA. **d** HAI antibody titers against H3N2 or H1N1 in serum were measured by HAI assay. An HAI antibody titer of 1:40 (red dotted line) was considered protective against influenza infection. **b**–**d** Data are expressed as dot plots, with horizontal lines representing the medians. **e** The mice were infected *i.n.* with 4 LD_{50} of H1N1 virus, and body weight and survival were monitored daily. Weight-loss data are shown as mean value ± SD. Survival data are represented as Kaplan–Meier survival curves. **b**–**d** Statistical analyses were performed using one-way ANOVA with Tukey's multiple comparisons or two-sided Mann–Whitney U test. This study was performed once. BW, body weight; N.D., not detected; ns, not significant. Source data are provided as a Source Data file.

between the vaccine and the circulating strain[47]. To overcome this problem, we hypothesized that the NVT-adjuvanted vaccine would be able to provide cross-protection against other mutated viruses that appear in different years, and we conducted the following experiment to confirm this hypothesis. As we cannot predict the strains that will be prevalent in the future, in this experiment, QIV from the 2020–2021 season was used as the vaccine, and the HAI titer and CD4⁺ T-cell responses were analyzed against the strains that were predicted to be prevalent that year for 3 years prior to the 2020–2021 season. The results showed that the serum HAI antibody titers against influenza strains different from the vaccine strain were overall low. In the group administered QIV *i.m.*, neutralizing antibodies against H3N2 or BV from the 2018–2019 season and against H3N2 from the 2019–2020 season were at very low levels or not produced at all. A similar trend was observed in the group administered QIV + NVT *i.n.*, which indicated that problems caused by antigenic mismatch cannot be solved by improving the vaccine adjuvant or administration route. In addition, in contrast to mice injected *i.m.* with QIV, which failed to induce T-cell responses in the lungs, mice administered QIV + NVT *i.n.* exhibited lung CD4⁺ T-cell responses to all the seasonal monovalent viral antigens tested (Fig. 8d). These results suggest that T-cell reactivity is less affected by antigenic drift than is neutralizing antibody reactivity and that a vaccine targeting lung CD4⁺ T_{RM} cells can provide a wider range of protection.

NVT-adjuvanted intranasal vaccine provides protection against heterosubtypic influenza virus infection in ferret model

Finally, we sought to explore whether the NVT-adjuvanted influenza vaccine is effective in ferrets, which are the optimal model for evaluating the pathogenicity of influenza viruses[48]. To test this hypothesis, ferrets were vaccinated *i.m.* with QIV or *i.n.* with QIV + NVT twice at two-week intervals, after which immunological analysis and challenge were performed. As expected, the serum HAI antibodies against H3N2 were similar between the two vaccine groups, and there were no neutralizing antibodies produced against H1N1 (Fig. 9a). Similar to our mouse studies, ferrets administered H3N2 + NVT *i.n.* had induced CD4⁺ T-cell responses to both H3N2 and H1N1 in the lung and spleen, whereas no T-cell responses were observed in ferrets administered H3N2 *i.m.* (Fig. 9b). To determine whether this immune response actually conveys protection, ferrets were infected *i.n.* with H1N1 virus, and virus titers were measured in nasal washes on days 0, 1, 3, and 5 post-infection. We found that the viral loads were lower in the group administered H3N2 + NVT via the intranasal route than in the group given H3N2 via the intramuscular route (Fig. 9c). Taken together, the principles of cross-protection that we verified in this study not only apply to mice but also apply to ferrets.

Discussion

Current injectable influenza vaccines are ineffective at protecting against antigenically mismatched strains that may lead to a pandemic as well as the seasonal flu epidemic[49]. Here, we showed that lung delivery of NVT-adjuvanted commercial QIV via the intranasal route provides cross-protection in various models. This vaccine induced mucosal antibody responses and promoted robust CD4⁺ T-cell responses in both the lung and spleen. Additionally, our vaccine induced the development of pulmonary CD4⁺ T_{RM} cells, which contributed to long-term broad protection. Mechanistic studies revealed that our vaccine conferred protective immunity in a type I IFN signaling-dependent manner.

In the present study, the addition of NVT to influenza vaccines increased the production of strain-specific neutralizing antibodies in serum. Furthermore, pulmonary delivery of the NVT-adjuvanted influenza vaccine induced mucosal antibody responses that were not induced by the injectable vaccine. In fact, mucosal antibodies are very effective at protecting against influenza virus at the site of initial infection[34]. We speculate that the NVT-adjuvanted pulmonary influenza vaccine likely provides better protection against vaccine-matched viral infection than conventional vaccines. It has been reported that mucosal IgA can provide broad cross-protection by reacting against multiple heterogeneous subtypes[50]. However, these cross-protective mucosal IgA antibodies appear to be applicable when targeting highly conserved regions of the neutralizing epitope, such as the HA stem or M2e domain[51,52]. In our study, mucosal antibodies alone did not prevent heterosubtypic virus infection without cross-reactive CD4⁺ T-cells. The reason may be that antigens in our vaccine do not target conserved neutralizing epitopes. If antigens targeting conserved neutralizing epitopes were to be added to our vaccine, the vaccine would be expected to show further improvement in efficacy because mucosal IgA can also contribute to cross-protection.

Because lung T_{RM} cells play a potent role in controlling respiratory infections, studies on the induction of lung T_{RM} cells through vaccination are attracting increased amounts of attention[11]. A fundamental approach to establish the lung T_{RM} cell pool is to drive cognate antigen recognition in the lung[9]. Here, we demonstrated that the administration volume of the vaccine is important in terms of the amount of vaccine that reaches the lungs via the intranasal route and that T_{RM} formation is possible only when the vaccine fully reaches the lungs (Supplementary Fig. 8 and Supplementary Fig. 9). In fact, administration of the vaccine via the intratracheal route through a catheter may be most effective for delivery to the lungs, but this method has practical limitations. Thus, we showed that intranasal or intratracheal administration of the NVT-adjuvanted vaccine generated similar levels of pulmonary CD4⁺ T_{RM} cells (Supplementary Fig. 10). Consistent with our findings, previous studies have also shown that delivery of a vaccine via the intranasal or intratracheal route rather than via the intramuscular or subcutaneous route induces pulmonary T_{RM} formation[20,53]. Another approach for the induction of T_{RM} cells is the "prime and pull" strategy, which involves a combination of systemic priming and mucosal boosting[11]. A recent study showed that immunization of mice by intramuscular priming and intranasal boost with the COVID-19 vaccine generated T_{RM} cells in the lungs and nasal mucosa[54]. Induction of lung T_{RM} cells by prime pool immunization was also confirmed by the results of a virus-like particle influenza vaccine study[55]. In the present study, pulmonary delivery of the NVT-adjuvanted vaccine after systemic priming through the intramuscular route generated lung T_{RM} cells. We also demonstrated that the use of NVT-adjuvanted antigen should be boosted because T_{RM} cells are not formed following boosting with the antigen or NVT alone.

https://doi.org/10.1038/s41467-024-54620-4

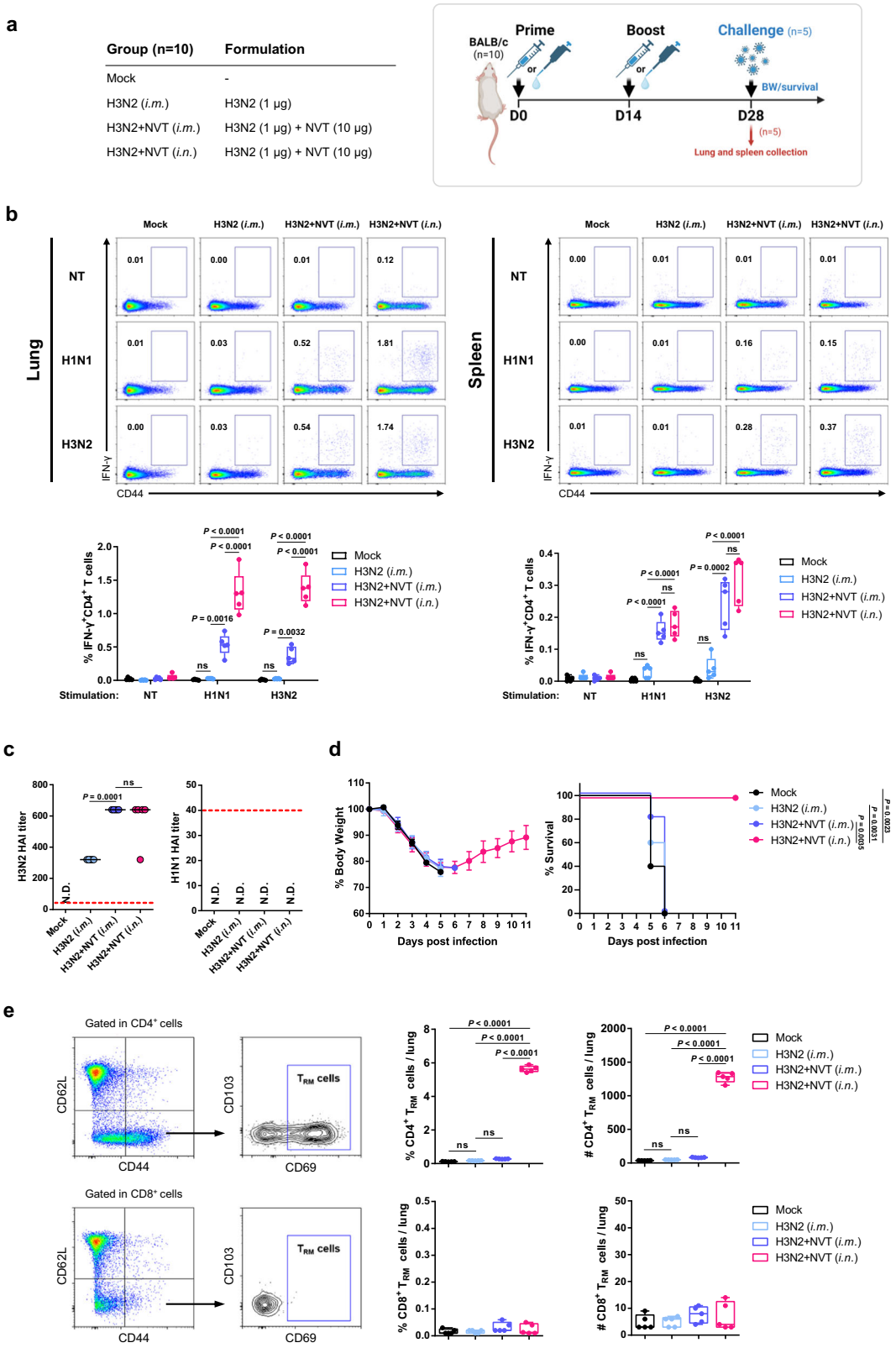

Overall, when the NVT-adjuvanted vaccine is delivered to the lungs of persons receiving the seasonal influenza vaccine, it may provide long-term and broad protection through the development of pulmonary T_{RM} cells. The proposed pulmonary vaccines used in these studies can be developed and co-exist with the conventional intramuscular vaccines as specific boosting vaccines when the circulating viral strains are not matched with the vaccine strains. Moreover, the long-term memory of the booster vaccine indicates that the vaccine does not need to be a regular seasonal vaccination but a sporadic vaccination (Supplementary Fig. 5).

The first step in the development of lung T_{RM} cells is the entry of activated antigen-specific T-cells into lung tissue by cytokines and chemokines[11]. We showed that pulmonary delivery of the NVT-adjuvanted vaccine induced the expression of various chemokines,

Fig. 4 | The CD4⁺ T-cell response in the lung, not in the spleen, plays a critical role in cross-protection against heterosubtypic influenza virus. a Experimental design. BALB/c mice (n = 10 per group) were immunized twice *i.m.* with H3N2 or H3N2 + NVT, or *i.n.* with H3N2 + NVT at two-week intervals. Two weeks after the last immunization, immune response analysis (n = 5 per group) (**b**, **c**, **e**) and H1N1 virus (A/Korea/2785/2009) challenge (n = 5 per group) (**d**) were performed. Schematic image was created in BioRender. Han, S. (2024) BioRender.com/e21s192. **b** After stimulating lung and spleen cells with H1N1 or H3N2, the IFN-γ⁺CD4⁺ T-cell response was determined by flow cytometry. **c** HAI antibody titers against H3N2 or H1N1 in serum were measured by HAI assay. An HAI antibody titer of 1:40 (red dotted line) was considered protective against influenza infection. **d** Mice were *i.n.* infected with 4 LD_{50} of H1N1 virus, and body weight and survival were monitored daily. Weight-loss data are shown as mean value ± SD. Survival data are represented as Kaplan–Meier survival curves, and the significant differences in survival rates were calculated by the log-rank test. **e** The proportion and number of CD4⁺ T_{RM} cells ($CD4^+CD44^+CD62L^-CD69^+$) and CD8⁺ T_{RM} cells ($CD8^+CD44^+CD62L^-CD69^+$) in the lungs were determined by flow cytometry. The gating strategy, frequency, and absolute number are shown. **b**, **e** Box and whisker plots show the median (center), 25th and 75th percentiles (box), and lowest and highest values (whiskers). **b**, **c**, **e** Statistical analyses were performed using one-way ANOVA with Tukey's multiple comparisons test. This study was performed independently at least three times, and one representative set is shown. BW, body weight; N.D., not detected; ns, not significant; NT, non-treated. Source data are provided as a Source Data file.

including CXCL9 and CXCL10. The chemokines CXCL9 and CXCL10 are generally known to play roles in regulating the differentiation of naïve T-cells into Th1 cells and pulling CXCR3⁺ effector T-cells to the local area[41]. Exploiting these roles, this set of chemokines is applicable to the prime and pull methods following vaccination. One report demonstrated that the administration of these chemokines after priming strongly recruited circulating activated effector CD8⁺ T-cells into local tissues[42]. Likewise, it is likely that the chemokines induced by the NVT-adjuvanted vaccine in this study promoted the recruitment of effector memory T-cells to the lungs, leading to the development of pulmonary T_{RM} cells. Despite our findings that chemokines are induced by NVT and not by the antigen, NVT alone fails to pull effector CD4⁺ T-cells into the lung, although there seems to be a slight increase in the CD4⁺ T_{RM} population (Fig. 6d). We have demonstrated the conditions underlying the formation of the CD4⁺ T_{RM} population by our adjuvant platform. However, further studies are needed to determine whether the signaling required to establish a T_{RM} population differs between CD4⁺ and CD8⁺ T-cells or whether the lung environment plays special roles in forming the T_{RM} population.

Our vaccine failed to induce lung CD4⁺ T_{RM} cells in IFNAR1$^{-/-}$ mice. One of the major reasons may be the reduced expression of chemokines. We found that levels of the chemokines CCL2, CCL5, CXCL9, and CXCL10, which directly affect CD4⁺ T-cell differentiation and migration[39–41], were significantly decreased in IFNAR1$^{-/-}$ mice. In fact, CCL2, CCL5, and CXCL10 have been reported to be induced by type I IFNs[41,56,57]. However, whether CXCL9 is directly regulated by type I IFNs is not fully understood. One review stated that CXCL9 is induced by IFN-γ but not by type I IFNs[41]. In contrast, one study showed that IFN-α/β also induces CXCL9, although not to the extent of IFN-γ[58]. In our study, we observed that CXCL9 was induced in a type I IFN signaling-dependent manner. Therefore, type I IFNs induced by NVT are important for the induction of chemokines that play an important role in the formation of protective immunity.

The majority of T-cell epitopes for influenza A virus are HA and NP proteins[59]. Since the NP of the influenza virus is a highly conserved antigen across influenza viruses (3), it has become a major target for T-cell-based influenza vaccines (4). Multiple studies have demonstrated that NP-based influenza vaccines provide protection against heterologous and homologous virus infections[60,61]. In the present study, mice immunized *i.n.* with H3N2 rNP, but not H3N2 rHA, together with NVT were able to survive heterosubtypic H1N1 virus challenge due to cross-reactive lung CD4⁺ T-cell responses. In fact, analyses using MHC tetramers can be used for accurate measurement of antigen-specific T-cell responses[62]. However, in this study, a commercial vaccine product was used as an antigen instead of tetramers for the following reasons: First, we sought to show this principle with a clinically relevant antigen. Second, we sought to test whether this principle could be reproduced in other strains, as well as in other animal species in addition to mice. Finally, identification of conserved epitopes is important for viral mutation and clinical translational research, but even if the corresponding epitope is found in mice, it is difficult to apply to humans owing to MHC restriction. Instead, we measured both T_{RM} and antigen-specific T-cell responses in the same lung cells to verify the antigen specificity of lung T_{RM} cells generated by our vaccine. In the future, research on the corresponding epitopes in humans can be completed through clinical trials.

Many studies have reported the possibility of T-cell-mediated immunopathology in the lung. CD8⁺ T-cells are a double-edged sword: they play an important role in viral clearance from the respiratory tract while also causing immunopathology[31]. Additionally, CD8⁺ T_{RM} cell responses can cause severe immunopathology and chronic pulmonary sequelae[13]. Dysregulated Th17 cells are also known to drive lung inflammation and autoimmune diseases[63]. In this study, intranasal vaccination with the NVT-adjuvanted vaccine did not cause excessive production of inflammatory cytokines in mice (Supplementary Fig. 11), likely because the vaccine did not induce uncontrolled Th17 and CTL responses in either the lung or spleen (Supplementary Fig. 1). In the future, clinical application of NVT-adjuvanted intranasal vaccines should be further validated for possible safety issues.

T-cell-based vaccines have become an emerging trend because they can provide broad immunity against variants that evade pre-existing neutralizing antibodies[64]. In the absence of virus-specific neutralizing antibodies, the T-cell response serves to reduce the worsening of the disease through viral clearance rather than preventing viral invasion[65]. From this perspective, the initial weight loss in mice that received the NVT-adjuvanted vaccine when infected with a lethal dose of heterosubtypic virus is thought to be due to the lack of protection against viral infection by neutralizing antibodies. Considering that the amount of virus that humans are exposed to in aerosols is usually low and not enough to cause illness[66], it is expected that the disease can be more easily controlled before progressing to serious symptoms through the T-cell-mediated immune response induced by vaccines. Indeed, the fact that universal influenza vaccines based on these systemic cellular responses are already in clinical trials[67,68] indicates that vaccines based on cellular immunity can work. In particular, a peptide-based vaccine targeting T-cells, flu-v, was confirmed to have some protective efficacy in phase 2b clinical trials[68]. If the vaccine antigens used in those studies were loaded into the platform described in this study, its effectiveness could be improved through the induction of lung T_{RM} cells. In other words, this vaccine platform prevents disease rather than preventing infection, especially when specialized for respiratory pathogens. Additionally, the cross-protective cellular immune response found in this work could be further harnessed to induce correlated protection and contribute to the development of a universal influenza vaccine[69–71].

Previously, we demonstrated that NVT remains stable even under accelerated conditions but rapidly degrades upon injection into the body, potentially minimizing the risk of side effects associated with prolonged presence in the body[32]. In addition, GLP toxicity studies conducted on various animal models, in accordance with OECD guidelines, confirmed that NVT is a safe substance that does not cause serious side effects when administered through the intramuscular or subcutaneous routes[32]. However, since intranasal administration of drugs can also cause both intended pharmacological and unintended

https://doi.org/10.1038/s41467-024-54620-4

a

Mice	Group (n=9)	Formulation
WT / KO	Mock	-
WT / KO	H3N2+NVT (*i.n.*)	H3N2 (1 μg) + NVT (10 μg)
KO	H1N1 (*i.m.*)	H1N1 (1 μg)

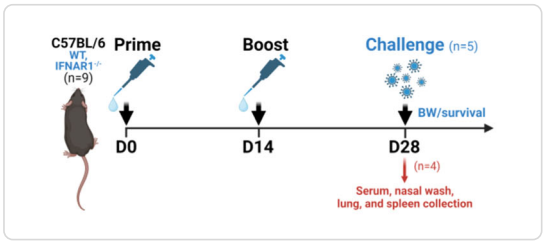

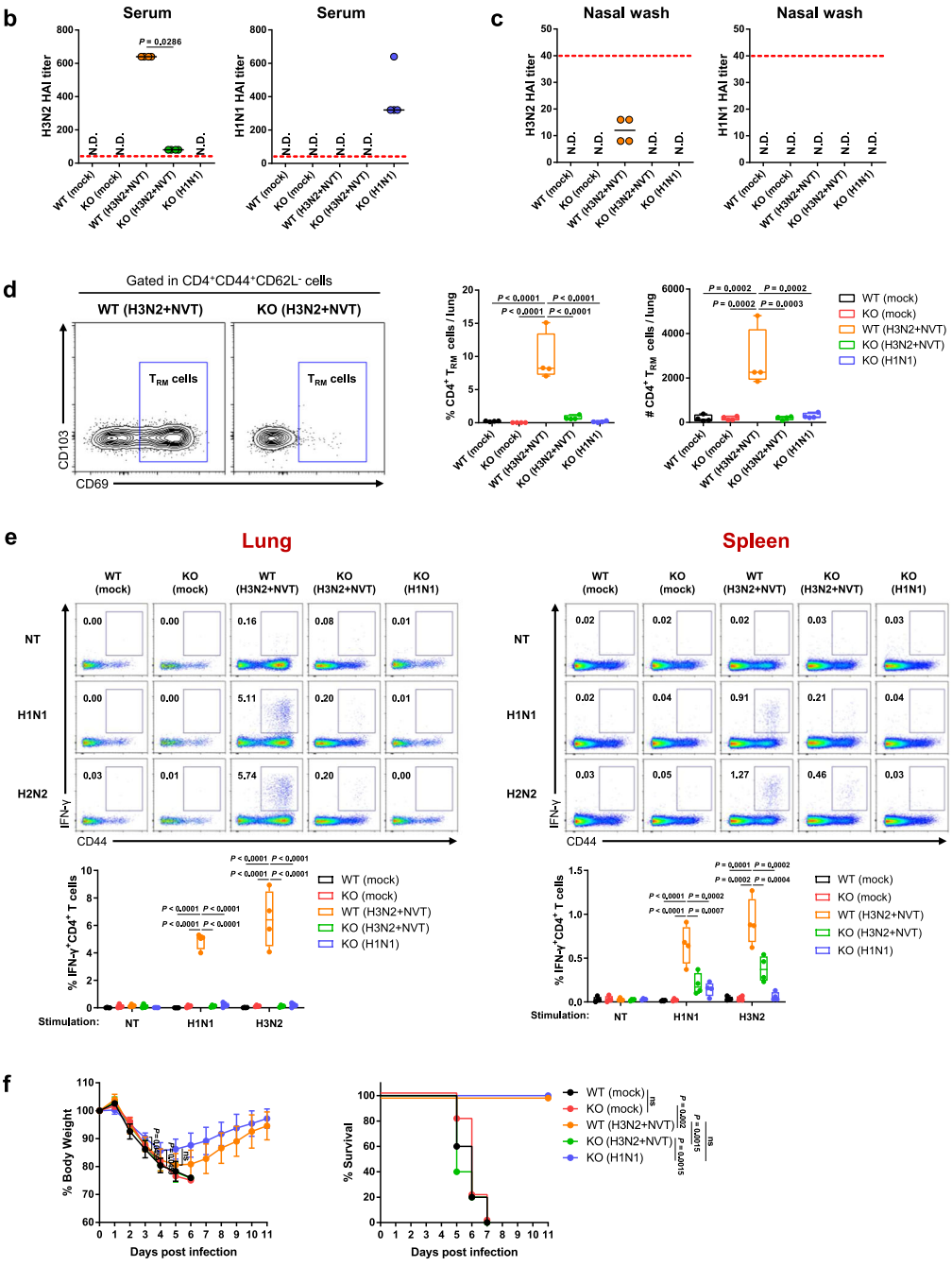

toxic effects[72], the safety of intranasal administration of NVT should be verified to address safety issues such as pulmonary toxicity.

In conclusion, we developed a vaccine platform that induces lung CD4$^+$ T_{RM} cells as a key target to provide long-lasting and broad coverage. Our findings hold important implications for public health, particularly for vaccines targeting respiratory pathogens. In the future, additional research will be necessary to apply a vaccine platform targeting lung T_{RM} cells to other infectious respiratory diseases, as well as lung cancer, in which cell-mediated immunity plays a critical role.

Methods

Ethics statement

All animal research was carried out in strict accordance with the recommendations of the Guide for the Care and Use of Laboratory

Fig. 5 | Type I IFN signaling is essential for the induction of protective immunity by the NVT-adjuvanted intranasal influenza vaccine. a Experimental design. WT (n = 9 per group) and IFNAR1$^{-/-}$ mice (n = 9 per group) were immunized *i.n.* with H3N2 + NVT twice at two-week intervals. Two weeks after the last immunization, immune response analysis (n = 4 per group) (**b**–**e**) and H1N1 virus (A/Korea/2785/2009) challenge (n = 5 per group) (**f**) were performed. Schematic image was created in BioRender. Han, S. (2024) BioRender.com/l89f720. **b**, **c** HAI antibody titers against H3N2 or H1N1 in (**b**) serum and (**c**) nasal washes were determined by HAI assay. An HAI antibody titer of 1:40 (red dotted line) was considered protective against influenza infection. **b**, **c** Data are expressed as dot plots, with horizontal lines representing the medians. **d**, **e** (**d**) The lung CD4$^+$ T_{RM} population and (**e**) CD4$^+$ T-cell responses to H1N1 or H3N2 in the lung and spleen were determined by using flow cytometry. Box and whisker plots showing the median (center), 25th and 75th percentiles (box), and lowest and highest values (whiskers). **f** The vaccinated mice were infected *i.n.* with 4 LD_{50} of H1N1 virus, and body weight and survival were monitored daily. Weight-loss data are shown as mean value ± SD. Survival data are represented as Kaplan–Meier survival curves, and the significant differences in survival rates were calculated by the log-rank test. **b**–**f** Statistical analyses were performed using one-way ANOVA with Tukey's multiple comparisons test or two-sided Mann–Whitney U test. This study was performed independently at least three times, and one representative set is shown. BW, body weight; N.D., not detected; ns, not significant; NT, non-treated. Source data are provided as a Source Data file.

Animals of the National Institutes of Health. Mouse studies were conducted with the approval of the Ethics Committee and Institutional Animal Care and Use Committee (Approval Number: NAVI-2021-0002) of the NAVI. Ferret studies were reviewed and approved by HLB Bio-Step (Approval Number: BIOSTEP IACUC 23-KE-0289).

Reagents and mice

The antibodies and seasonal inactivated influenza vaccines used in this study are listed in Tables S1 and S2, respectively. Influenza vaccines were kindly provided by Il-Yang Pharmaceutical (Yongin, Korea). Four monovalent vaccines from the 2020-2021 influenza season were used in the mouse study, and the H3N2 monovalent vaccine from the 2022-2023 influenza season was used in the ferret study. The QIV contained equal proportions of the four strains from the 2020–2021 influenza season. The recombinant HA (Cat no. 40789-V08H) and NP (Cat no. 40778-V08B) of H3N2 (A/Cambodia/e0826360/2020) and the recombinant HA (Cat no. 11684-V08H) and NP (Cat no. 11675-V08B) of H1N1 (A/Puerto Rico/8/1934) were purchased from Sino Biological (Beijing, China). Specific pathogen-free C57BL/6 and BALB/c female mice at 6 weeks of age were purchased from Samtako Bio Korea (Kyounggi, Korea), and type I IFN receptor 1-deficient (IFNAR1$^{-/-}$) mice on the C57BL/6 background were kindly provided by Prof. Jae-Ho Cho (Chonnam National University Medical School, Korea). All mice were housed with food and water *ad libitum* in the animal facility of the NA Vaccine Institute (Seoul, Korea).

Cells and viruses

Madin-Darby canine kidney (MDCK) cells (CCL-34, ATCC) were maintained in Minimum Essential Eagle's Medium (Welgene, Korea) supplemented with 10% heat-inactivated fetal bovine serum and 1% penicillin/streptomycin. BALB/c mouse-adapted influenza A/Korea/2785/2009 (H1N1) strains were obtained from the Korea Disease Control and Prevention Agency (Cheongju, Chungcheongbuk-do, Korea). Pandemic influenza A/Puerto Rico/8/1934 (PR8, H1N1) was purchased from ATCC. Influenza B/Shandong/7/97 (Victoria lineage, BV) was kindly provided by Prof. Baik Lin Seong (Yonsei University, Seoul, Korea). The human influenza A/Victoria/2570/2019 (H1N1) strain was kindly provided by Il-Yang Pharmaceutical. Canine influenza A/canine/VC378/2012 (H3N2) was kindly provided by Prof. Woon-Sung Na (Chonnam National University, Gwangju, Korea). Influenza viruses were propagated in MDCK cells or fertile chicken eggs and quantified via a plaque assay. The 50% lethal dose (LD_{50}) was determined by infecting mice with serial dilutions of the virus.

Vaccine preparation

Influenza viruses propagated in fertilized eggs were subjected to gradient centrifugation to remove impurities from the fertilized eggs. The collected liquid was treated with Triton X-100 and stirred for 1 hour at room temperature to split the influenza virus. Then, Triton X-100 was removed while adding PBS using the Cogent M1 TFF system. The purified influenza viruses were inactivated with 0.01% formaldehyde, and the inactivation of viruses was confirmed by serial passages via eggs or plaque assays. The final influenza monovalent vaccines were prepared through a sterilizing filtration process.

Production of NVT

NVT was produced as previously described in ref. 32. Briefly, the nucleotide segment (1,701-2,112; 412 nucleotides) from the Chinese sacbrood virus genome was cloned and inserted into the pUC-GW-Amp vector and amplified by the polymerase chain reaction. Single-stranded RNAs (ssRNAs) complementary to the PCR products were synthesized via in vitro transcription and subsequently annealed into dsRNAs. NVT was ultimately obtained through ethanol purification after DNase I and RNase T1 treatment of the dsRNA.

Plaque assay

MDCK cells were seeded at 5×10^5 cells per well in a six-well plate and infected with 10-fold serially diluted virus or lung extracts for 1 h. After the inocula were removed, the cells were overlaid with medium containing 1% agarose and 2 μg/ml of TPCK-treated trypsin (Sigma–Aldrich, St. Louis, MO) and incubated for 48–72 h at 37 °C in an atmosphere of 5% CO_2. When plaques were visible, the cells were fixed with 4% paraformaldehyde and stained with 0.1% crystal violet solution (Sigma–Aldrich, St. Louis, MO), after which the plaques were counted.

Plaque reduction neutralization test (PRNT)

MDCK cells were seeded at 5×10^5 cells per well in a six-well plate and incubated overnight at 37 °C in an atmosphere of 5% CO_2 until approximately 95% confluence was reached. Test and control serum samples were serially diluted 2-fold starting from 1:1. The H1N1 virus was prepared by diluting the virus in serum-free medium to generate 50 to 100 plaques in virus control wells. An equal volume of virus was added to the diluted serum and incubated for 1 h at 37 °C in an atmosphere of 5% CO_2 to allow for neutralization. After the virus-serum inoculum was removed, the wells were overlaid with medium containing 1% agarose and 2 μg/ml TPCK-treated trypsin and incubated until plaques were formed. Viral plaques were visualized by fixing cells with 4% paraformaldehyde and staining with 0.1% crystal violet solution. The $PRNT_{50}$ titer was defined as the reciprocal of the highest serum dilution that inhibited more than 50% of the plaque relative to the viral control.

Immunization and viral challenge

In this study, 50 μl of material was injected into the mice of the intramuscular group, and 30 μl of material was administered to the intranasal group via the intranasal route for delivery to the lungs (Supplementary Fig. 8). To investigate the overall profile of QIV according to the route of administration and addition of NVT, BALB/c mice (female, 6-8 weeks old) were immunized intramuscularly (*i.m.*) with QIV (4 μg) or intranasally (*i.n.*) with QIV or adjuvanted with NVT (10 μg) (QIV + NVT) twice at two-week intervals. Two weeks after the last immunization, the mice were sacrificed for immune response analysis or challenged *i.n.* with 100 LD_{50} or 5,000 LD_{50} of the H1N1 virus (A/Korea/2785/2009).

https://doi.org/10.1038/s41467-024-54620-4

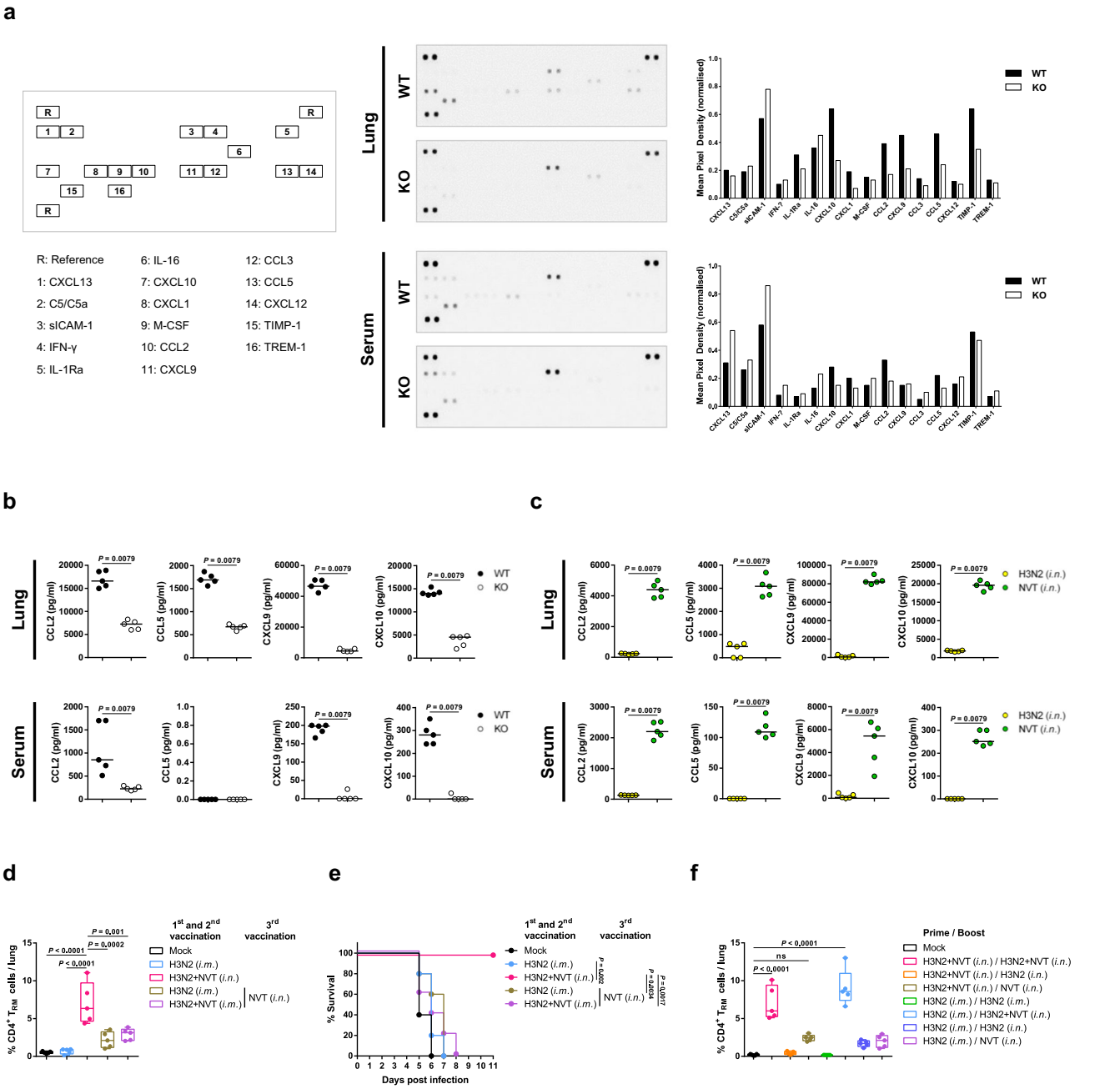

Fig. 6 | Chemokines induced by NVT contribute to lung CD4$^+$ T_{RM} cell formation, but direct codelivery of antigens is essential. a, **b** WT (n = 5) and IFNAR1$^{-/-}$ mice (n = 5) were immunized *i.n.* with NVT + H3N2. One day later, lung lysates and serum were collected. **a** Pooled lung lysates and serum samples were analyzed using a mouse cytokine kit. The signals were normalized to the pixel density of the indicated reference spots. **b** Concentrations of CCL2, CCL5, CXCL9, and CXCL10 in lung lysates and sera were measured via ELISA. **c** BALB/c Mice (n = 5 per group) were immunized *i.n.* with H3N2 or NVT. One day later, the levels of CCL2, CCL5, CXCL9, and CXCL10 in lung lysates and sera were assessed via ELISA. **b**, **c** Data are expressed as dot plots, with horizontal lines representing the medians. The two-sided Mann–Whitney U test was used for statistical analysis of differences between two groups. **d**, **e** BALB/c mice were immunized *i.m.* with H3N2 (n = 20), H3N2 + NVT (n = 10), or *i.n.* with H3N2 + NVT (n = 10) twice at two-week intervals. Two weeks later, mice injected *i.m.* with H3N2 (n = 10) or H3N2 + NVT (n = 10) were boosted *i.n.* with NVT. **d** On day 42, the proportion of lung CD4$^+$ T_{RM} cells from vaccinated mice (n = 5 per group) was determined via flow cytometry. **e** The other vaccinated mice (n = 5 per group) were infected *i.n.* with 4 LD_{50} of H1N1 virus, and survival was monitored daily. Survival data are represented as Kaplan–Meier survival curves, and the significant differences in survival rates were calculated by the log-rank test. **f** BALB/c mice were immunized *i.n.* with H3N2 + NVT (n = 15) or *i.m.* with H3N2 (n = 20). Two weeks later, the mice were immunized *i.m.* with H3N2 or *i.n.* with H3N2 + NVT, H3N2, or NVT, and the proportion of lung CD4$^+$ T_{RM} cells was determined via flow cytometry on day 42. **d**, **f** Box and whisker plots showing the median (center), 25th and 75th percentiles (box), and lowest and highest values (whiskers). Statistical analyses were performed using one-way ANOVA with the Tukey's multiple comparisons test. This study was performed once. ns, not significant. Source data are provided as a Source Data file.

For the cross-protection study, BALB/c mice were immunized *i.m.* with H3N2 (1 μg) or *i.n.* with H3N2 adjuvanted with NVT (10 μg) (H3N2 + NVT) twice at two-week intervals. To examine which T-cell responses, local or systemic, contributed to cross-protection, BALB/c mice were immunized *i.m.* with H3N2, H3N2 + NVT or *i.n.* with H3N2 + NVT twice at two-week intervals. To determine the vaccine components contributing to cross-protection, BALB/c mice were immunized *i.n.* with 1 μg of recombinant H3N2 HA, NP, or whole

https://doi.org/10.1038/s41467-024-54620-4

a

Group (n=9)	Formulation
Mock	-
H3N2 rHA	H3N2 rHA (1 μg) + NVT (10 μg)
H3N2 rNP	H3N2 rNP (1 μg) + NVT (10 μg)
H3N2	H3N2 (1 μg) + NVT (10 μg)

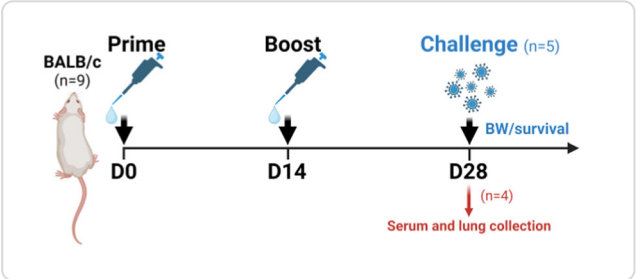

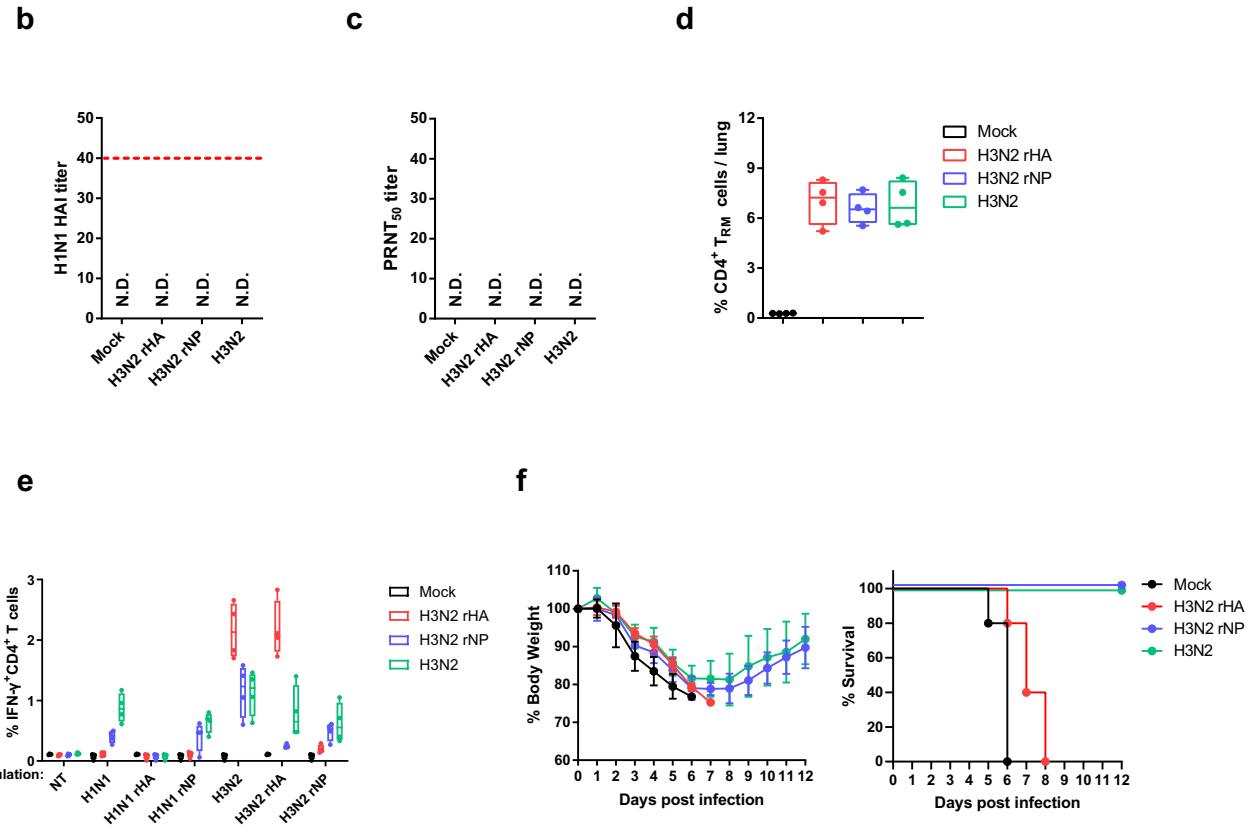

Fig. 7 | The influenza NP is a conserved CD4 epitope source for cross-protection. a Experimental design. BALB/c mice (n = 9 per group) were immunized *i.n.* with NVT-adjuvanted recombinant H3N2 HA (H3N2 rHA), recombinant H3N2 NP (H3N2 rNP), or H3N2 (whole vaccine) twice at two-week intervals. Two weeks after the last immunization, immune response analysis (n = 4 per group) (**b**–**e**) and H1N1 virus (A/Korea/2785/2009) challenge (n = 5 per group) (**e**) were performed. Schematic image was created in BioRender. Han, S. (2024) BioRender.com/l62g951. **b, c** (**b**) The HAI titer and (**c**) $PRNT_{50}$ titer against H1N1 virus in serum were measured. **d** Lung $CD4^+$ T_{RM} cells were evaluated by flow cytometry. **e** After stimulating the lung cells with H1N1, H1N1 rHA, H1N1 rNP, H3N2, H3N2 rHA, or H3N2 rNP, IFN-γ^+CD4^+ T-cell response was determined via flow cytometry. **d**, **e** Box and whisker plots showing the median (center), 25th and 75th percentiles (box), and lowest and highest values (whiskers). **f** Mice were infected *i.n.* with 4 LD_{50} of H1N1 virus, and body weight and survival were monitored daily. Weight-loss data are shown as mean value ± SD. Survival data are represented as Kaplan–Meier survival curves. This study was performed once. BW body weight, N.D. not detected, NT non-treated. Source data are provided as a Source Data file.

H3N2 vaccine in combination with NVT (10 μg) twice at two-week intervals. To study whether the protective immunity induced by the NVT-adjuvanted vaccine depends on type I IFN signaling, wild-type (WT) or $IFNAR1^{-/-}$ mice were immunized *i.n.* with H3N2 + NVT twice at two-week intervals. Two weeks after these vaccinations, immune responses were analyzed, or the mice were challenged *i.n.* with 4 LD_{50} of H1N1 (A/Korea/2785/2009) virus. For the $CD4^+$ T-cell depletion experiment, mice were given 200 μg of anti-CD4 (GK1.5) monoclonal antibody intraperitoneally two weeks after the second vaccination, three times for one week, and then challenged.

To study cross-protection against type B influenza virus, BALB/c mice were immunized *i.m.* with BV (1 μg), BY (1 μg) or *i.n.* with BV + NVT or BY + NVT twice at two-week intervals and infected *i.n.* with 4 LD_{50} of BV (B/Shandong/7/97) virus. To study the cross-protective effects of type A and B influenza viruses, BALB/c mice were immunized *i.m.* with H1N1 (1 μg), BY (1 μg) or *i.n.* with H1N1 + NVT or BY + NVT twice at two-week intervals and challenged *i.n.* with 4 LD_{50} of H1N1 (A/Korea/2785/2009). To explore cross-protection against viruses of different origins, mice were immunized *i.m.* with 1 μg of H3N2 or *i.n.* with H3N2 + NVT twice at two-week intervals and infected *i.n.* with 10 LD_{50} of canine H3N2 (A/canine/VC378/2012) virus. In all challenge experiments, mice

https://doi.org/10.1038/s41467-024-54620-4

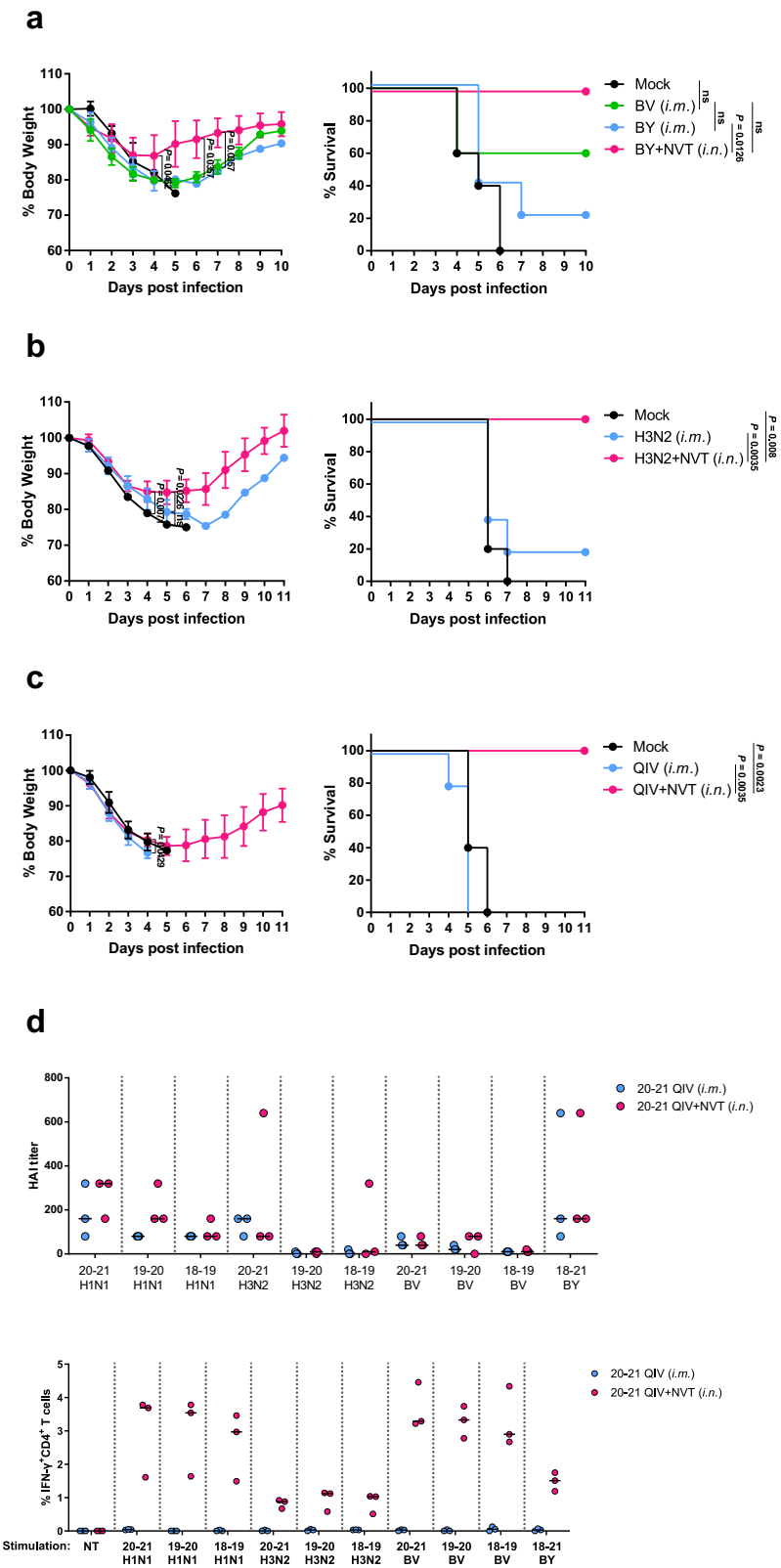

that lost 25% of their initial body weight were euthanized and recorded as dead.

Determination of influenza virus-specific antibodies

Influenza virus-specific total IgG, IgG1, and IgG2a antibodies in the serum or IgA antibodies in the nasal wash and bronchoalveolar lavage fluid (BALF) were measured via enzyme-linked immunosorbent assays (ELISAs). To determine the vaccine-specific antibody titers of mouse samples relative to standard mouse IgG, wells for standard curves were coated with goat anti-mouse IgG antibody, and wells for samples were coated with the vaccine antigen used in the study in a 96-well immunoplate. After the plates were blocked with 1% skim milk, serially diluted mouse IgG antibodies (for the standards) or samples were added and incubated for 2 h at room

Fig. 8 | The principle of cross-protection was verified between the various subtypes. a Mice (n = 5 per group) were immunized *i.m.* with BV or BY, or *i.n.* with BY + NVT twice at two-week intervals. Two weeks after the last vaccination, the mice were *i.n.* challenged with BV virus (B/Shandong/7/97). Body weight and survival were monitored daily. **b** Mice (n = 5 per group) were immunized *i.m.* with H3N2 or *i.n.* with H3N2 + NVT twice at two-week intervals. Two weeks after the last vaccination, the mice were *i.n.* challenged with canine H3N2 virus (A/canine/VC378/2012). Body weight and survival were monitored daily. **c** Mice (n = 5 per group) were immunized *i.m.* with QIV or *i.n.* with QIV + NVT twice at two-week intervals. Two weeks after the last vaccination, the mice were *i.n.* challenged with pandemic H1N1 virus (A/Puerto Rico/8/34). Body weight and survival were monitored daily. **a**–**c** Weight-loss data are shown as mean value ± SD. Survival data are represented as Kaplan–Meier survival curves, and the significant differences in survival rates were calculated by the log-rank test. **d** Mice (n = 20 per group) were immunized *i.m.* with 2020-2021 season QIV, or *i.n.* with QIV + NVT twice at two-week intervals. Two weeks after the last immunization, pooled sera and pooled lung cells were used to measure the serum HAI titer and lung $CD4^+$ T-cell response to each indicated seasonal influenza vaccine strain. The data are expressed as dot plots, with horizontal lines representing the medians. These experiments were performed once. ns, not significant. Source data are provided as a Source Data file.

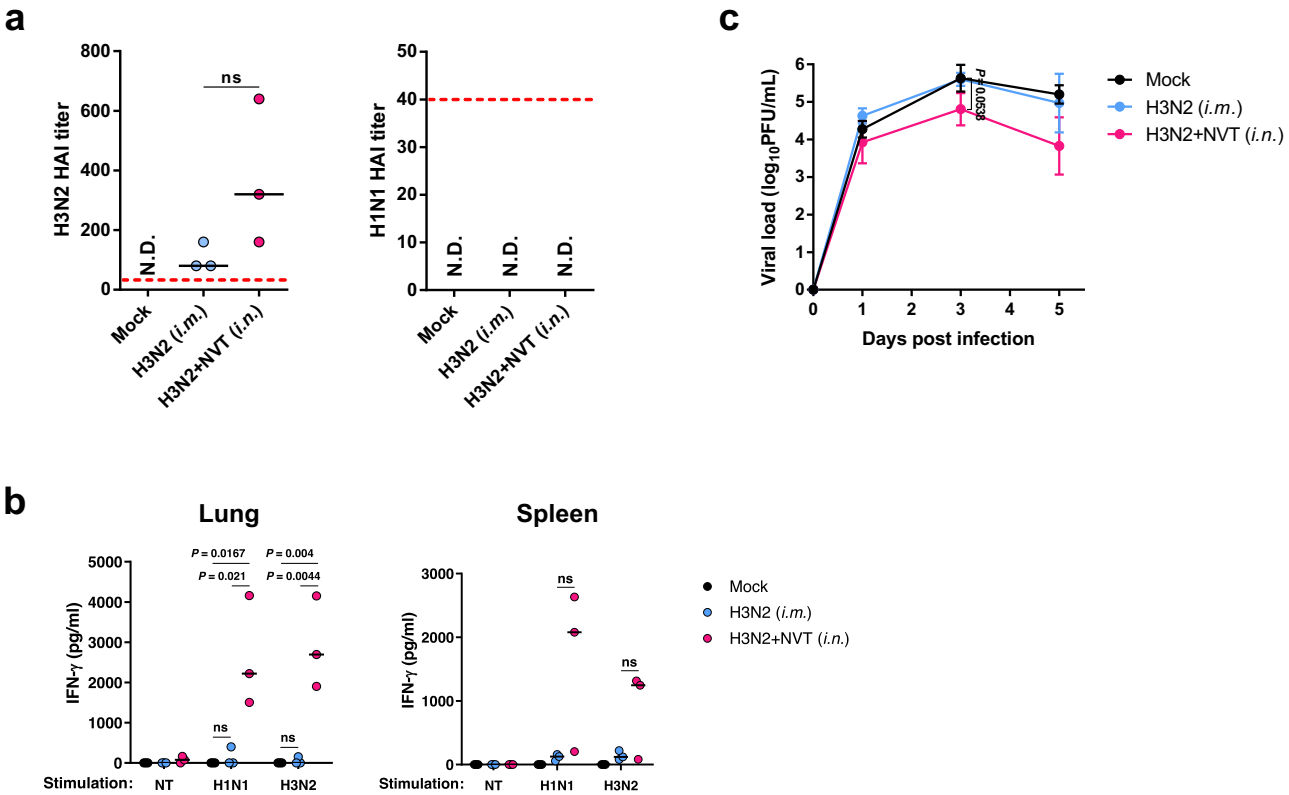

Fig. 9 | NVT-adjuvanted intranasal vaccine contributes to cross-protection in the ferret model. Ferrets (n = 6 per group) were vaccinated *i.m.* with H3N2 or *i.n.* with H3N2 + NVT twice at two-week intervals. Two weeks after the last immunization, immune response analysis (n = 3 per group) (**a**, **b**) and H1N1 virus (A/Korea/2785/2009) challenge (n = 3 per group) (**c**) were performed. **a** HAI antibody titers against H3N2 or H1N1 in serum were measured by HAI assay. An HAI antibody titer of 1:40 (red dotted line) was considered protective against influenza infection. **b** Lung and spleen cells were stimulated with H1N1 or H3N2 for 3 days, and the production of IFN-γ in the culture supernatant was measured using ELISA. **a**, **b** Data are expressed as dot plots, with horizontal lines representing the medians. **c** The vaccinated ferrets were infected *i.n.* with 1 × 107 PFU of H1N1 virus. Nasal wash samples were collected on days 0, 1, 3, and 5 post-challenge, and viral titers were determined using a plaque assay. Data are shown as mean value ± SD. **a**–**c** Statistical analyses were performed using one-way ANOVA with Tukey's multiple comparisons test or two-sided Mann–Whitney U test. The ferret study was performed independently three times, and one representative set is shown. N.D., not detected; ns, not significant. Source data are provided as a Source Data file.

temperature. After washing the plate, HRP-conjugated anti-mouse antibodies against IgG, IgG1, IgG2a, or IgA were added as secondary antibodies and incubated for 1 h at room temperature. The color in the wells was developed using 3,3′,5,5′-tetramethylbenzidine substrate solution (Sigma–Aldrich, St. Louis, MO) and stopped by the addition of 0.5 M HCl. The absorbance was read at 450–590 nm by a Multiskan Sky microplate reader (Thermo Fisher Scientific, Waltham, MA, USA). Antibody titers were calculated as arbitrary units relative to the standard curve.

Measurement of cytokines and chemokines

Relative levels of cytokines and chemokines in lung lysates and serum from vaccinated mice were determined by a Proteome Profiler Mouse Cytokine Array Kit (Panel A, R&D Systems, Minneapolis, MN, USA) in accordance with the manufacturer's recommendations. ImageJ software was used for the measurement of pixel density. The concentrations of cytokines (IL-1β, IL-6, and TNF-α) and chemokines (CCL2, CCL5, CXCL9, and CXCL10) in lung lysates and serum were measured using the appropriate ELISA kits.

Hemagglutination inhibition (HAI) assay

HAI titers were determined in serum, nasal wash, and BALF samples collected from vaccinated mice or from serum samples from vaccinated ferrets. All the samples were treated with receptor-destroying enzyme (RDE) and PBS at a 1:3:6 ratio overnight at 37 °C to remove nonspecific interference. Serum samples were inactivated at 56 °C for

30 min after RDE treatment. The samples were serially diluted 2-fold in a 96-well V-bottom plate, 4 hemagglutination units of H1N1 or H3N2 antigen were added to each well of the diluted serum sample, and the mixture was incubated at room temperature for 30 min. The mixture was then reacted with 1% chicken red blood cells for 30 min at room temperature, after which the presence of aggregation was evaluated. The HAI titer was expressed as the dilution factor of the highest serum dilution that completely inhibited hemagglutination. An HAI titer of 1:40 was considered to provide protection against influenza infection[69].

Flow cytometry

Lungs and spleens from vaccinated mice were harvested and dissociated into single cells. To examine antigen-specific T-cell responses, single-cell suspensions were stimulated with 5 μg/ml of the antigen used for vaccination overnight at 37 °C. Then, the protein transport inhibitor GolgiPlug (BD Bioscience, Franklin Lakes, NJ, USA) was added to the cells, which were further incubated for 4–6 h. After the Fc receptor was blocked with the CD16/CD32 antibody, the cells were subjected to live/dead staining with a fixable viability dye and surface staining with anti-mouse CD4, CD8a and CD44 antibodies. The cells were then fixed and permeabilized using Cytofix/Cytoperm solution (BD Bioscience) and stained intracellularly with anti-mouse IFN-γ, IL-4 and IL-17A antibodies. After washing, the cells were resuspended in FACS buffer (PBS containing 1% FBS and 0.1% NaN_3) and analyzed by flow cytometry. To analyze lung T_{RM} cell subsets, single lung cells were stained with surface antibodies specific for CD4, CD8a, CD44, CD62L, CD69, and CD103 and analyzed by flow cytometry.

Lung histopathology

For pathological examination, lungs isolated from mice at 6 dpi were fixed in 4% paraformaldehyde for 1–2 days and dehydrated sequentially in 20% and 30% sucrose in PBS at 4 °C until the tissues sank. After the lung tissues were embedded in OCT compound freezing medium (Leica Biosystems, Deer Park, IL, USA), the frozen samples were cut at 10 μm and mounted on silane-coated glass slides (Muto Pure Chemicals Co., Ltd., Tokyo, Japan). Conventional hematoxylin and eosin staining of the sectioned lung tissues was performed.

Acute Lung Injury (ALI) Scoring

Lung injury scoring of infected lungs was determined by a previously described method[73]. To assess the lung tissue, 20 images were randomly selected from scanned H&E stained sections of lung slides at 400x magnification using the digital pathology software QuPath. The evaluation includes scoring five parameters, each rated on a scale from 0 to 2. The parameters are as follows:

(A) Neutrophils in the alveolar space: none = 0, 1-5 = 1, or >5 = 2
(B) Neutrophils in the interstitial space: none = 0, 1-5 = 1, or >5 = 2
(C) Hyaline membranes: none = 0, 1 = 1, or >1 = 2
(D) Proteinaceous debris filling the airspaces: none = 0, 1 = 1, or >1 = 2
(E) Alveolar septal thickening: <2x = 0, 2x-4x = 1, or >4x = 2

The score for each field is computed where A through E represent the factors mentioned. The overall scores are obtained by adding the scores in each field. An overall score of zero suggests a healthy lung, while a score of 1 indicates severe acute lung injury. Scores are calculated using the following equation:

Score = (20 A + 14B + 7 C + 7D + 2E)/Total field number 20 * 100.

Ferret studies

Prior to this study, ferrets were confirmed to be seronegative by the HAI assay against the vaccine and challenge strains. For vaccination, healthy 1-year-old male ferrets were immunized *i.m.* with 1 ml of 2022–2023 seasonal H3N2 (20 μg) or *i.n.* with 1 ml (0.5 ml in each nostril) of H3N2 (20 μg) + NVT (100 μg) on days 0 and 14. On day 28, the lungs, spleens, and serum from vaccinated ferrets were collected. Sera were used for the HAI assay. Lung and spleen cells were stimulated with 5 μg/ml H1N1 (2022-2023 season) or H3N2 (2022-2023 season) and incubated for 3 days at 37 °C in a humidified atmosphere of 5% CO_2. The culture supernatants were used for the measurement of ferret IFN-γ. In a challenge study, ferrets were administered 10^7 PFU of H1N1 (A/Victoria/2570/2019) virus *i.n.*, and nasal wash samples were collected at 0, 1, 3, and 5 dpi.

Coomassie Staining and Western blot analysis

Two sets of QIV, H3N2, and H3N2 rNP were loaded onto 12% sodium dodecyl sulfate polyacrylamide gel electrophoresis (SDS-PAGE) gel. One set of gels was stained with Coomassie Protein Stain (Abcam, Cambridge, UK) for 30 min at room temperature. The other set of unstained gels was transferred onto nitrocellulose transfer membrane (GenDEPOT, Katy, TX, USA) using a tank transfer system (Bio-Rad, Hercules, CA, USA). Then, the membrane was washed with Tris-buffered saline containing Tween 20 (TBST), blocked with 5% skim milk, and incubated overnight with serum from H3N2 rNP-vaccinated mouse at 4 °C. After washing with TBST, the membrane was further incubated with HRP-conjugated anti-mouse IgG. The bands on the membrane were detected with ECL pico plus solution (DyneBio, South Korea). Reactive bands were detected by the Vilber Fusion FX (Vilber, France). Intensities of the bands were measured by ImageJ software.

Statistical analysis

Statistical analyses were performed using GraphPad Prism version 6.00 for Windows (GraphPad Software, La Jolla, CA, USA; www.graphpad.com). Comparisons between two groups were statistically evaluated using the nonparametric Mann–Whitney U test. Significant differences among multiple groups were determined using one-way analysis of variance (ANOVA) with Tukey's multiple comparison test.

Reporting summary

Further information on research design is available in the Nature Portfolio Reporting Summary linked to this article.

Data availability

The data that support the findings of this study are available within the paper (and supplementary information files). Source data are provided with this paper.

References

1. Nypaver, C., Dehlinger, C. & Carter, C. Influenza and Influenza Vaccine: A Review. *J. Midwifery Women's Health* **66**, 45–53 (2021).
2. Wei, C. J. et al. Next-generation influenza vaccines: opportunities and challenges. *Nat. Rev. Drug Discov.* **19**, 239–252 (2020).
3. Soema, P. C., Kompier, R., Amorij, J. P. & Kersten, G. F. Current and next generation influenza vaccines: Formulation and production strategies. *Eur. J. Pharm. Biopharm.* **94**, 251–263 (2015).
4. Gupta, D. & Mohan, S. Influenza vaccine: a review on current scenario and future prospects. *J. Genet Eng. Biotechnol.* **21**, 154 (2023).
5. Houser, K. & Subbarao, K. Influenza vaccines: challenges and solutions. *Cell Host Microbe* **17**, 295–300 (2015).
6. Berlanda Scorza, F., Tsvetnitsky, V. & Donnelly, J. J. Universal influenza vaccines: Shifting to better vaccines. *Vaccine* **34**, 2926–2933 (2016).
7. Barman, S., Soni, D., Brook, B., Nanishi, E. & Dowling, D. J. Precision Vaccine Development: Cues From Natural Immunity. *Front Immunol.* **12**, 662218 (2021).
8. Afkhami, S. et al. Respiratory mucosal delivery of next-generation COVID-19 vaccine provides robust protection against both ancestral and variant strains of SARS-CoV-2. *Cell* **185**, 896–915.e819 (2022).

9. Zheng, M. Z. M. & Wakim, L. M. Tissue resident memory T cells in the respiratory tract. *Mucosal Immunol.* **15**, 379–388 (2022).
10. Yuan, R. et al. The Roles of Tissue-Resident Memory T Cells in Lung Diseases. *Front Immunol.* **12**, 710375 (2021).
11. Qian, Y., Zhu, Y., Li, Y. & Li, B. Legend of the Sentinels: Development of Lung Resident Memory T Cells and Their Roles in Diseases. *Front Immunol.* **11**, 624411 (2020).
12. Zhang, M., Li, N., He, Y., Shi, T. & Jie, Z. Pulmonary resident memory T cells in respiratory virus infection and their inspiration on therapeutic strategies. *Front Immunol.* **13**, 943331 (2022).
13. Cheon, I. S., Son, Y. M., Sun, J. Tissue-resident memory T cells and lung immunopathology. *Immunol. Rev.* **316**, 63–83 (2023).
14. Grau-Exposito, J. et al. Peripheral and lung resident memory T cell responses against SARS-CoV-2. *Nat. Commun.* **12**, 3010 (2021).
15. Hogan, R. J. et al. Activated antigen-specific CD8+ T cells persist in the lungs following recovery from respiratory virus infections. *J. Immunol.* **166**, 1813–1822 (2001).
16. Son, Y. M. et al. Tissue-resident CD4(+) T helper cells assist the development of protective respiratory B and CD8(+) T cell memory responses. *Sci. Immunol.* **6**, eabb6852 (2021).
17. Teijaro, J. R. et al. Cutting edge: Tissue-retentive lung memory CD4 T cells mediate optimal protection to respiratory virus infection. *J. Immunol.* **187**, 5510–5514 (2011).
18. Takamura, S. et al. Specific niches for lung-resident memory CD8+ T cells at the site of tissue regeneration enable CD69-independent maintenance. *J. Exp. Med* **213**, 3057–3073 (2016).
19. Teijaro, J. R., Verhoeven, D., Page, C. A., Turner, D. & Farber, D. L. Memory CD4 T cells direct protective responses to influenza virus in the lungs through helper-independent mechanisms. *J. Virol.* **84**, 9217–9226 (2010).
20. Uddback, I. et al. Long-term maintenance of lung resident memory T cells is mediated by persistent antigen. *Mucosal Immunol.* **14**, 92–99 (2021).
21. Slutter, B. et al. Dynamics of influenza-induced lung-resident memory T cells underlie waning heterosubtypic immunity. *Sci. Immunol.* **2**, eaag2031 (2017).
22. Zhao, J. et al. Airway Memory CD4(+) T Cells Mediate Protective Immunity against Emerging Respiratory Coronaviruses. *Immunity* **44**, 1379–1391 (2016).
23. Channappanavar, R., Fett, C., Zhao, J., Meyerholz, D. K. & Perlman, S. Virus-specific memory CD8 T cells provide substantial protection from lethal severe acute respiratory syndrome coronavirus infection. *J. Virol.* **88**, 11034–11044 (2014).
24. Misplon J. A., Lo C. Y., Crabbs T. A., Price G. E., Epstein S. L. Adenoviral-vectored universal influenza vaccines administered intranasally reduce lung inflammatory responses upon viral challenge 15 months post-vaccination. *J. Virol.* **97**, e0067423 (2023).
25. Madhavan, M. et al. Tolerability and immunogenicity of an intranasally-administered adenovirus-vectored COVID-19 vaccine: An open-label partially-randomised ascending dose phase I trial. *EBioMedicine* **85**, 104298 (2022).
26. Gilchuk, P. et al. A Distinct Lung-Interstitium-Resident Memory CD8(+) T Cell Subset Confers Enhanced Protection to Lower Respiratory Tract Infection. *Cell Rep.* **16**, 1800–1809 (2016).
27. Rakhra, K. et al. Exploiting albumin as a mucosal vaccine chaperone for robust generation of lung-resident memory T cells. *Sci. Immunol.* **6**, eabd8003 (2021).
28. Wosen, J. E., Mukhopadhyay, D., Macaubas, C. & Mellins, E. D. Epithelial MHC Class II Expression and Its Role in Antigen Presentation in the Gastrointestinal and Respiratory Tracts. *Front Immunol.* **9**, 2144 (2018).
29. Goplen, N. P. et al. Tissue-resident CD8(+) T cells drive age-associated chronic lung sequelae after viral pneumonia. *Sci. Immunol.* **5**, eabc4557 (2020).
30. Puzyrenko, A. et al. Cytotoxic CD8-positive T-lymphocyte infiltration in the lungs as a histological pattern of SARS-CoV-2 pneumonitis. *Pathology* **54**, 404–408 (2022).
31. Schmidt, M. E. et al. Memory CD8 T cells mediate severe immunopathology following respiratory syncytial virus infection. *PLoS Pathog.* **14**, e1006810 (2018).
32. Ko, K. H. et al. A novel defined TLR3 agonist as an effective vaccine adjuvant. *Front Immunol.* **14**, 1075291 (2023).
33. Lee, S.-H. et al. The Defined TLR3 Agonist, Nexavant, Exhibits Anti-Cancer Efficacy and Potentiates Anti-PD-1 Antibody Therapy by Enhancing Immune Cell Infiltration. *Cancers* **15**, 5752 (2023).
34. van Riet, E., Ainai, A., Suzuki, T. & Hasegawa, H. Mucosal IgA responses in influenza virus infections; thoughts for vaccine design. *Vaccine* **30**, 5893–5900 (2012).
35. Painter, M. M. et al. Rapid induction of antigen-specific CD4(+) T cells is associated with coordinated humoral and cellular immunity to SARS-CoV-2 mRNA vaccination. *Immunity* **54**, 2133–2142.e2133 (2021).
36. Tseng, H. F. et al. Effectiveness of mRNA-1273 against SARS-CoV-2 Omicron and Delta variants. *Nat. Med* **28**, 1063–1071 (2022).
37. Zens, K. D. & Farber, D. L. Memory CD4 T cells in influenza. *Curr. Top. Microbiol Immunol.* **386**, 399–421 (2015).
38. Meyts, I. & Casanova, J. L. Viral infections in humans and mice with genetic deficiencies of the type I IFN response pathway. *Eur. J. Immunol.* **51**, 1039–1061 (2021).
39. Bakos, E. et al. CCR2 Regulates the Immune Response by Modulating the Interconversion and Function of Effector and Regulatory T Cells. *J. Immunol.* **198**, 4659–4671 (2017).
40. Hu, J. Y. et al. Increasing CCL5/CCR5 on CD4+ T cells in peripheral blood of oral lichen planus. *Cytokine* **62**, 141–145 (2013).
41. Tokunaga, R. et al. CXCL9, CXCL10, CXCL11/CXCR3 axis for immune activation - A target for novel cancer therapy. *Cancer Treat. Rev.* **63**, 40–47 (2018).
42. Shin, H. & Iwasaki, A. A vaccine strategy that protects against genital herpes by establishing local memory T cells. *Nature* **491**, 463–467 (2012).
43. Nuwarda, R. F., Alharbi, A. A. & Kayser, V. An Overview of Influenza Viruses and Vaccines. *Vaccines (Basel)* **9**, 1032 (2021).
44. Luo, J. et al. Induction of cross-protection against influenza A virus by DNA prime-intranasal protein boost strategy based on nucleoprotein. *Virol. J.* **9**, 286 (2012).
45. Moin, S. M. et al. Co-immunization with hemagglutinin stem immunogens elicits cross-group neutralizing antibodies and broad protection against influenza A viruses. *Immunity* **55**, 2405–2418.e2407 (2022).
46. Hancock, K. et al. Cross-reactive antibody responses to the 2009 pandemic H1N1 influenza virus. *N. Engl. J. Med* **361**, 1945–1952 (2009).
47. Lewnard, J. A. & Cobey S. Immune History and Influenza Vaccine Effectiveness. *Vaccines (Basel)* **6**, 28 (2018).
48. Belser, J. A. et al. A Guide for the Use of the Ferret Model for Influenza Virus Infection. *Am. J. Pathol.* **190**, 11–24 (2020).
49. Keshavarz, M. et al. Influenza vaccine: Where are we and where do we go? *Rev. Med Virol.* **29**, e2014 (2019).
50. Muramatsu, M. et al. Comparison of antiviral activity between IgA and IgG specific to influenza virus hemagglutinin: increased potential of IgA for heterosubtypic immunity. *PLoS One* **9**, e85582 (2014).
51. Guthmiller, J. J. et al. Broadly neutralizing antibodies target a haemagglutinin anchor epitope. *Nature* **602**, 314–320 (2022).
52. Deng, L., Cho, K. J., Fiers, W. & Saelens, X. M2e-Based Universal Influenza A Vaccines. *Vaccines (Basel)* **3**, 105–136 (2015).
53. Perdomo, C. et al. Mucosal BCG Vaccination Induces Protective Lung-Resident Memory T Cell Populations against Tuberculosis. *mBio* **7**, e01686-16 (2016).

54. Diallo, B. K. et al. Intranasal COVID-19 vaccine induces respiratory memory T cells and protects K18-hACE mice against SARS-CoV-2 infection. *NPJ Vaccines* **8**, 68 (2023).
55. Hodgins, B., Pillet, S., Landry, N. & Ward, B. J. Prime-pull vaccination with a plant-derived virus-like particle influenza vaccine elicits a broad immune response and protects aged mice from death and frailty after challenge. *Immun. Ageing* **16**, 27 (2019).
56. Lehmann, M. H. et al. CCL2 expression is mediated by type I IFN receptor and recruits NK and T cells to the lung during MVA infection. *J. Leukoc. Biol.* **99**, 1057–1064 (2016).
57. Nakano, M. et al. Type I interferon induces CX3CL1 (fractalkine) and CCL5 (RANTES) production in human pulmonary vascular endothelial cells. *Clin. Exp. Immunol.* **170**, 94–100 (2012).
58. Antonelli, A. et al. Interferon-alpha, -beta and -gamma induce CXCL9 and CXCL10 secretion by human thyrocytes: modulation by peroxisome proliferator-activated receptor-gamma agonists. *Cytokine* **50**, 260–267 (2010).
59. Bui, H. H., Peters, B., Assarsson, E., Mbawuike, I. & Sette, A. Ab and T cell epitopes of influenza A virus, knowledge and opportunities. *Proc. Natl Acad. Sci. USA* **104**, 246–251 (2007).
60. Zheng, M. et al. Cross-protection against influenza virus infection by intranasal administration of nucleoprotein-based vaccine with compound 48/80 adjuvant. *Hum. Vaccin Immunother.* **11**, 397–406 (2015).
61. Guo, L. et al. Protection against multiple influenza A virus subtypes by intranasal administration of recombinant nucleoprotein. *Arch. Virol.* **155**, 1765–1775 (2010).
62. Kurtulus, S. & Hildeman, D. Assessment of CD4(+) and CD8 (+) T cell responses using MHC class I and II tetramers. *Methods Mol. Biol.* **979**, 71–79 (2013).
63. Lei, L. et al. Th17 cells and IL-17 promote the skin and lung inflammation and fibrosis process in a bleomycin-induced murine model of systemic sclerosis. *Clin. Exp. Rheumatol.* **34**, 14–22 (2016).
64. Kingstad-Bakke, B. et al. Vaccine-induced systemic and mucosal T cell immunity to SARS-CoV-2 viral variants. *Proc. Natl Acad. Sci. USA* **119**, e2118312119 (2022).
65. Arieta, C. M. et al. The T-cell-directed vaccine BNT162b4 encoding conserved non-spike antigens protects animals from severe SARS-CoV-2 infection. *Cell* **186**, 2392–2409.e2321 (2023).
66. Yezli, S. & Otter, J. A. Minimum Infective Dose of the Major Human Respiratory and Enteric Viruses Transmitted Through Food and the Environment. *Food Environ. Virol.* **3**, 1–30 (2011).
67. Leroux-Roels, I. et al. Immunogenicity, safety, and preliminary efficacy evaluation of OVX836, a nucleoprotein-based universal influenza A vaccine candidate: a randomised, double-blind, placebo-controlled, phase 2a trial. *Lancet Infect. Dis.* **23**, 1360–1369 (2023).
68. Pleguezuelos, O. et al. Efficacy of FLU-v, a broad-spectrum influenza vaccine, in a randomized phase IIb human influenza challenge study. *NPJ Vaccines* **5**, 22 (2020).
69. Paules, C. I., Marston, H. D., Eisinger, R. W., Baltimore, D. & Fauci, A. S. The Pathway to a Universal Influenza Vaccine. *Immunity* **47**, 599–603 (2017).
70. Jang, Y. H. & Seong, B. L. Call for a paradigm shift in the design of universal influenza vaccines by harnessing multiple correlates of protection. *Expert Opin. Drug Discov.* **15**, 1441–1455 (2020).
71. Jang, Y. H. & Seong, B. L. The Quest for a Truly Universal Influenza Vaccine. *Front Cell Infect. Microbiol* **9**, 344 (2019).
72. Emami, A. et al. Toxicology Evaluation of Drugs Administered via Uncommon Routes: Intranasal, Intraocular, Intrathecal/Intraspinal, and Intra-Articular. *Int J. Toxicol.* **37**, 4–27 (2018).
73. Matute-Bello, G. et al. An official American Thoracic Society workshop report: features and measurements of experimental acute lung injury in animals. *Am. J. Respir. Cell Mol. Biol.* **44**, 725–738 (2011).

Acknowledgements

We thank members of the NA Vaccine Institute for insightful discussion and Prof. Jae-Ho Cho (Chonnam National University Medical School, Korea) for providing IFNAR1$^{-/-}$ mice. This research was supported by a grant from the Korea Health Technology R&D Project through the Korea Health Industry Development Institute (KHIDI), funded by the Ministry of Health & Welfare (RS-2022-KH128236 and RS-2022-KH128243, Republic of Korea), and supported by Korea Drug Development Fund funded by Ministry of Science and ICT, Ministry of Trade, Industry, and Energy, and Ministry of Health & Welfare (RS-2024-00337146, Republic of Korea).

Author contributions

S.B.C. and D.-H.K. conceived the study. S.B.C., S.H.H., and K.H.K. designed the experiments. K.H.K., H.S.B., J.W.P., J.-S.L., S.P., J.H.., H.P., J.C., E.B., and S.-H.P. performed the experiments and data analysis. W.N. and B.-L.S. provided important reagents. S.H.H. and D.-H.K. provided critical comments. KHK and SBC wrote and reviewed the manuscript. All the authors contributed to the article and approved the submitted version.

Competing interests

K.H.K., H.S.B., D.-H.K., and S.B.C. are employees of the NA Vaccine Institute Research and Development Center. J.H. and H.P. are employees of Il-Yang Pharmaceutical. The remaining authors declare no competing interests.

Additional information

Supplementary information The online version contains supplementary material available at https://doi.org/10.1038/s41467-024-54620-4.

Correspondence and requests for materials should be addressed to Dong-Ho Kim or Seung Bin Cha.

Peer review information *Nature Communications* thanks Yoshikazu Honda-Okubo, Katherine Kedzierska, and the other, anonymous, reviewer for their contribution to the peer review of this work. A peer review file is available.